CORRELATION BETWEEN AMBIENT AIR TEMPERATURE AND EFFECTIVE BRIDGE TEMPERATURE BASED ON LONG-TERM FIELD MONITORING: A CASE STUDY OF A CONCRETE GIRDER BRIDGE IN SOUTH AFRICA

Jurie F. Adendorff[1]; Sarah A. Skorpen, Ph.D.[2]; Elsabé P. Kearsley, Ph.D.[3]

[1]Ph.D. Candidate, Department of Civil Engineering, University of Pretoria, Private Bag X20, Hatfield 0028, South Africa (corresponding author). ORCID: https://orcid.org/0000-0003-4125-1271. Email: jurie.adendorff@tuks.co.za

[2]Senior Lecturer, Department of Civil Engineering, University of Pretoria, Private Bag X20, Hatfield 0028, South Africa. ORCID: https://orcid.org/0000-0003-4151-2179. Email: sarah.skorpen@up.ac.za

[3]Professor, Department of Civil Engineering, University of Pretoria, Private Bag X20, Hatfield 0028, South Africa. ORCID: https://orcid.org/0000-0003-0458-8908. Email: elsabe.kearsley@up.ac.za

ABSTRACT

This study investigates the long-term thermal behavior of a reinforced concrete twin spine-beam bridge, the Van Zylspruit Bridge, located in central South Africa. This research utilizes nine years of field monitoring data, including over 11.5-million data points from 41 thermistors as well as local meteorological information, to establish appropriate design correlations between the environment and the bridge's thermal response.

The study found that the temperature specifications for both Ambient Air Temperature (AAT) and Effective Bridge Temperature (EBT) in the South African Bridge Code, TMH 7, were overly conservative for this specific bridge and location. For instance, the design 50-year return period

minimum and maximum AAT corresponded to actual return periods of 3 675 years and 595 years, respectively. Similarly, the design EBT limits showed significantly longer actual return periods. Ultimately, this study underscores the critical importance of using appropriate thermal material properties alongside locally relevant environmental data for thermal design of bridges and proposes an adapted method for determining design effective bridge temperatures based on local meteorological data.

INTRODUCTION

Reinforced concrete (RC) bridges are subjected to many loading conditions including live loads due to traffic and continuously occurring environmental loads such as thermal variation. Thermal strain from temperature variation in the deck is often the largest contributor to lateral bridge deck movement, however, it has been reported that it is often neglected in the design of bridges (Hoffman and Phares, 2014) or is under designed (Saad et al., 2023). The three main mechanisms of heat transfer experienced by a bridge deck during thermal loading are radiation, convection and conduction (Potgieter and Gamble, 1989; Saad et al., 2023; Saad et al., 2025). These mechanisms are dependent of factors such as geographic location, time of day, season, climatological conditions, material properties and geometry, such as cross-section geometry (Elbadry and Ghali, 1983; Priestley, 1978; Saad et al., 2023; Saad et al., 2025). The mechanisms of heat transfer result in various temperature distributions that may occur within a bridge such as a uniform temperature across the entire section as well as linear and nonlinear temperature gradients in both the horizontal and vertical directions (Saad et al., 2025). These temperature distributions result in a variety of movements of the bridge deck both during construction and the continuous service life of the bridge (Saad et al., 2025; Song et al., 2016). Movement of the bridge deck induced by thermal loading are usually accommodated by the provision of joints or the inclusion of bearings (Elbadry and Ghali, 1983; Priestley, 1978; Dreyer et al., 2025).

However, in the case of integral bridges, thermally induced movements are restrained by the monolithic deck-abutment connection and can result in significant load effects (Dreyer et al., 2025). Thermally induced stresses are an important design consideration since they have been found to:

(1) exacerbate the effects of live loads (Pearson et al., 2024);

(2) be comparable to that caused by live loads (Zhou et al., 2021); or

(3) may even be higher than that of live loads (Li et al., 2023).

BACKGROUND

To better understand the thermal behaviour of bridges, researchers have resolved to the field monitoring of bridges exposed to environmental loading. Black et al. (1976) were able to derive bridge deck temperatures from the measured deck movement of seven concrete bridges in the UK, one of which was continuously monitored for 5 years (the Hammersmith Flyover). They found that the mean Effective Bridge Temperature (EBT), defined as the weighted average temperature across the cross-section (Black et al., 1976), over a period of five days could be taken as being equal to the mean ambient air temperature (AAT) over the same period. A five-day mean AAT or EBT, referred to as a mean pentad, is the average of five consecutive daily maximum and minimum temperatures. Their results are displayed in **Fig. 1**. The EBT could further be defined as an equivalent uniform temperature that represents the structural thermal state for analysis and design purposes. It reflects how heat is absorbed, stored, and conducted within the bridge's materials (concrete, steel, asphalt, etc.), often lagging behind daily ambient fluctuations.

Black et al. (1976) further suggested that "*Since there appears to be a reasonable agreement between measured effective bridge temperatures and effective bridge temperatures estimated from the range of mean pentads plus a daily swing, it seems reasonable to assume that the effective bridge temperature at any time can be deduced in a similar way, assuming that the annual mean effective bridge temperature and annual mean shade temperature are the same"* (Black et al., 1976). According to Black et al. (1976), this could be used for bridge maintenance purposes, such as setting expansion joints since the EBT governs the longitudinal movement due to thermal expansion (Skorpen et al., 2019).

Black et al. (1976) also established a correlation between the daily change in Effective Bridge Temperature (ΔTEBT) and the area-to-width ratio of a concrete bridge deck, as depicted in **Fig. 2**. The area-to-width ratio refers to the ratio between the cross-sectional area of the bridge deck to the width of the bridge deck, effectively representing the equivalent height of the bridge deck. Therefore, the cross-sectional shape of the bridge deck has an impact on ΔT_{EBT}, as is evident in **Fig. 2**.

Black et al. (1976) observed an exponential decline in daily change in EBT as the area-to-width ratio increased in concrete bridge decks, a trend supported by other authors (Emerson, 1976; Skorpen,

2020; Skorpen et al., 2020). From **Fig. 2** it can be seen that the numerical models produced by Skorpen (2020) follow the same trend as the results of Black et al. (1976) and Emerson (1976), however at slightly elevated temperatures. This is mostly due to the difference in thermal loading input. Skorpen (2020) applied thermal loading representative of hot and arid conditions situated in South Africa, which are more severe than those applied by authors using thermal loading representative of UK climatology (Black et al., 1976; Emerson, 1976).

Emerson (1976) investigated the relationship between the AAT and EBT and proposed a method for determining design temperature magnitudes for EBT. They obtained data from five field monitored concrete bridges over a span of nine years and AAT data from the nearest meteorological stations. From the data they first established a correlation between the daily (24-hour) minimum and the two-day (48-hour) mean AAT. Thereafter they established a correlation between the two-day (48-hour) mean AAT and the daily (24-hour) minimum EBT, therefore, indirectly relating daily EBT to daily AAT. The results of these correlations are shown in **Fig. 3** from which a design procedure was derived to determining the design minimum EBTs, as indicated by the red arrows in the figure. The procedure starts by first identifying a suitable minimum 24-hour AAT obtained from 50-year return period minimum AAT isochromes of the UK. To illustrate the design procedure, a 24-hour minimum AAT of 0 ℃ can be assumed. From the right side of the figure, the 48-hour mean AAT corresponding to a 24-hour minimum AAT of 0 ℃ is 4 ℃. The 48-hour mean AAT of 4 ℃ can be linked to the figure on the left side, providing a corresponding 24-hour minimum EBT of 4.5 ℃, as indicated by the red arrow. Therefore, the design minimum EBT to be used for a concrete bridge would be 4.5 ℃ in this instance. A similar method was proposed for determining the 24-hour maximum EBT. This design procedure has been adopted by the British Standards Institution document on bridge loading at the time (BS 5400, 1978) as well as by the TMH 7 design code (TMH 7, 1989) which was used for designing the Van Zylspruit Bridge in South Africa.

Saad et al. (2023) and Saad et al. (2025) performed numerical analyses to investigate the effect of climate change on the vertical thermal gradients of concrete box girders. They used various climactic prediction models to extrapolate potential anomalous climate conditions, such as heat waves, cold fronts and periods of maximum daily temperature variations, to 1000 years in the future. They found that the

projected increase in thermal differentials may have a significant effect on the condition and life cycle of a bridge, such as possible increases in tensile strain, fatigue and deformations. However, they reported that the effect of climate change on the temperature gradient in the concrete box girders was highly dependent on the climactic prediction model used as well as on the geographical location for which the climate was extrapolated. It is therefore important to consider the appropriate climatological conditions when designing bridges.

Reinforced concrete bridges in Southern Africa, such as the Van Zylspruit (VZ) Bridge, are subject to design principals based on climatological conditions from the UK, using isotherms for South Africa. This is partly due to the lack of appropriate long-term data establishing relations between the climate and thermal behaviour of RC bridges in Southern Africa. With the advent of digital instrumentation, long-term remote field monitoring of Southern African bridges has become possible. This study aims to leverage data from long-term field monitoring to establish appropriate design correlations between the environment and RC bridge thermal behaviour of the Van Zylspruit Bridge, located in central South Africa. This can allow designers to define more accurate deck movements, enabling longer bridge spans, more reliable soil backfill pressure assessments and more efficient maintenance.

FIELD MONITORING

The Van Zylspruit Bridge

The Van Zylspruit Bridge (**Fig. 4**) is a 90.6m-long RC integral bridge, constructed in South Africa between 2015 and 2016, located 113 km South of Bloemfontein on the N1 Highway. The bridge consists of five spans with a 1m-deep twin spine-beam cross-section. A detailed construction sequence and instrumentational setup is available in Skorpen (2020). The Van Zylspruit Bridge is located in a hot and arid region of central South Africa, at a latitude of -29.99° S, which bears significant influence on the thermal behaviour of the bridge (Potgieter and Gamble, 1989).

A durability specification concrete (40 MPa compressive cube strength) was used for the VZ bridge, the mix design of which can be found in Skorpen (2020). The concrete had a measured thermal expansion coefficient (α) between 8.5 and 9.75 x10^{-6}/°C. Additional material properties can be found in Skorpen (2020).

Previous research presented on the VZ Bridge mostly focused on the data collected during the first three years after construction (Skorpen et al., 2018; Skorpen et al., 2019; Skorpen, 2020). Skorpen et al. (2020) examined the correlation between ambient temperatures and the effective temperatures experienced by the bridge deck and how they affect the corresponding abutment movement and earth pressures behind the abutments. Findings revealed that the deck was subjected to approximately 60 % to 70 % of the temperature variation considered in design calculations for 2016 and 2017. Consequently, the resulting thermal movements were significantly smaller than originally expected. They further reported that the abutment movement was governed by the change in effective temperature of the uncracked bridge deck cross-section. In turn, the change in daily effective temperature of the uncracked deck cross-section corresponded well with the findings of Black et al. (1976) and Emerson (1976), as indicated in **Fig. 2**, in that with an increase in cross-sectional area per unit width of deck, a decrease in effective deck temperature occurs.

This study aimed to investigate the correlation between the environment and thermal behaviour of the VZ bridge to establish design parameters appropriate to the local climatological conditions. The study leveraged the long-term monitored temperature data obtained from the 41 thermistors installed in the bridge deck, as shown in **Fig. 5**, each recording at a sampling interval of 15 minutes for nine years post-construction, resulting in over 11.5-million raw data points.

Climatological Conditions

Meteorological data was obtained from the nearest weather station to the VZ bridge, recorded in hourly increments continuously since 2015 (Moeletsi et al., 2022). The recorded ambient air temperature (AAT), solar radiation (SR), wind speed (WS) and wind direction (WD) are displayed in **Fig. 6** and the descriptive statistics is shown in **Table 1**. The gap in the data (July 2020 to July 2021) was due to technical difficulties experienced at the weather station due to imposed lockdown restrictions during the Covid-19 pandemic.

Although the study focuses primarily on temperature, the climatological parameters were documented to contextualise the local climate at the Van Zylspruit Bridge. For example, rainfall can influence ambient air temperature and, in turn, the effective bridge temperature. This broader

perspective is consistent with Potgieter and Gamble (1989), who linked climatological conditions to stresses in bridges.

The ambient air temperature typically varied between a 5th percentile recorded temperature of 1.8 ℃ and a 95th percentile of 29.5 ℃, giving a typical yearly temperature range of 31.3 ℃. The mean AAT and standard deviation were calculated as 15.5 ℃ and 8.3 ℃, respectively. The 50-year return period for the upper (40 ℃) and lower (-13 ℃) limit for the AAT as specified by TMH 7 is shown in **Fig. 6**. The probability (P) for the AAT to be equal to, or exceed, the TMH 7 upper limit, P(AAT $\geqslant$ TMH 7 Upper Limit) = 0.17 %, which corresponds to a return period of 595 years. Similarly for the lower limit, P(AAT $\leq$ TMH 7 Lower Limit) = 0.03 %, which corresponds to a return period of 3 675 years. The AAT range specified by TMH 7 is 53 ℃ and has a 0.07 % probability of being exceeded, which corresponds to a return period of 1 429 years. When considering the calculated limits for various return periods, as shown in **Fig. 7**, along with the actual return periods for the TMH 7 AAT limits, it is clear that the limits specified by TMH 7 is overly conservative. The calculated AAT limits for a 50-year return period is -1.4 ℃ for the lower limit and 32.7 ℃ for the upper limit, resulting in a temperature range of 34.1 ℃ which is 35.7 % lower than the TMH 7 specified temperature range. The AAT limits are important to consider since it forms the basis for determining the EBT in design codes like TMH 7.

During the summer (December to February), the AAT typically varied between 16.4 ℃ and 32.2 ℃ with a mean value and standard deviation of 21.3 ℃ and 6.3 ℃, respectively. The solar radiation typically exceeded 1 000 W/m^2 at midday. During the winter (June to August), the AAT typically varied between 3.4 ℃ and 19.9 ℃ with a mean value and standard deviation of 8.6 ℃ and 6.7 ℃, respectively. The solar radiation typically exceeded 600 W/m^2 at midday. A comparison of solar radiation at VZ and the UK during the "hot summer of 1976" (**Fig. 8**) shows that summer solar radiation at VZ is typically much higher than during the summer of the UK, which is more akin to VZ's winter.

The minimum and maximum recorded ambient temperatures for the entire monitored period was -10.0 ℃ and 39.9 ℃. The maximum recorded solar radiation was 1 219 W/m2. The maximum daily solar radiation for different return periods is shown in **Fig. 7**. The calculated 50-year return period for maximum daily solar radiation is 1 273 W/m^2.

The mean hourly wind speeds for summer, autumn, winter and spring were 3.2 m/s, 2.7 m/s, 3.0 m/s and 3.2 m/s, respectively, indicating that summer and spring are the windiest seasons, followed by winter and autumn. However, the highest recorded wind speed of 15.1 m/s was recorded in the winter of 2019. From the wind rose in **Fig. 6** it can be seen that the overall dominant wind direction is North-West followed by a North North-Westerly direction. The mean daily wind speed for different return periods is shown in **Fig. 7**. The 50-year return period for mean daily wind speed is 6.0 m/s, further indicating the low wind speeds of the region.

Fig. 9 shows the recorded relative humidity (RH) and daily rainfall. Their descriptive statistics can be found in **Table 1**. The highest and lowest mean relative humidity was in autumn (58.8 %) and spring (40.6 %), respectively. The region experienced a drought during the construction of the bridge which ended in February 2017 when over 200 mm of rain fell (Skorpen, 2020), which is evident in **Fig. 9**. Since then, the average yearly rainfall measured 457 mm with the most rainfall occurring in 2022 at 879 mm. Rainfall appeared to impact humidity levels during the construction period, as the substantial precipitation in February 2017 led to an increase in humidity compared to the previous year (Skorpen, 2020) as seen in **Fig. 9**. From **Table 1** the seasonal rainfall shows the mean rainfall for summer, autumn, winter and spring to be 189 mm, 138 mm, 29 mm, and 77 mm, respectively. It is clear that the most and least amount of rainfall is expected to be during summer and winter, respectively. All the abovementioned climactic factors influence the thermal behaviour of concrete bridges (Elbadry and Ghali, 1983; Song et al., 2016; Saad et al., 2025).

The climatological conditions described at the VZ bridge such as low wind speeds combined with high solar radiation create conditions for significant temperature differentials, potentially leading to high stress levels and cracking (Potgieter and Gamble, 1989). These conditions contradict the milder and colder conditions experienced in the UK, which were used to formulate the design procedure used for the VZ Bridge. The UK typically experiences lower AATs as well as lower temperature ranges combined with lower solar radiation (below 900 W/m^2 in the summer) and higher rainfall than at the VZ bridge (Emerson, 1977; Emerson, 1980).

Effective Bridge Temperature

The recorded thermistor data was used to calculate the Effective Bridge Temperature of the twin spine-beam using the method described by Black et al. (1976) and is shown in **Fig. 10** for nine years post-construction. A 6-month gap between 2019 and 2020 can be observed in the data due to the solar panels being stolen (Morley et al., 2025). The descriptive statistics of the EBT is shown in **Table 2**.

The EBT for the past nine years ranged from a minimum of 2.6 ℃ to a maximum of 36.5 ℃ with an average yearly maximum temperature difference of 31.9 ℃ (standard deviation, σ, of 0.97 ℃). This is merely 66.5 % of the design annual temperature difference of 46 ℃ as specified by TMH 7 (TMH 7, 1989), which is obtained from the difference between the maximum and minimum design temperatures of 38 ℃ and -8 ℃, respectively and shown in **Fig. 10**. This corresponds with the findings of Skorpen et al. (2018), Skorpen et al. (2019), Skorpen (2020) and Skorpen et al. (2020) for the 3-year period post-construction. The probability of the EBT to be equal to, or exceed, the TMH 7 specifications is P(EBT ⩾ TMH 7 Upper Limit) = 0.42 % which corresponds to a 238-year return period for the upper limit and P(EBT ⩽ TMH 7 Lower Limit) = 0.01 % which corresponds to a 10 000-year return period for the lower limit. The probability of the annual EBT range to exceed 46 ℃ is 0.07 % which corresponds to a 1 429-year return period. From the calculated EBT limits for various return periods as shown in **Fig. 11**, it is clear that the design specifications were conservative. The calculated EBT limits for a 50-year return period is 4.3 ℃ for the lower limit and 33.8 ℃ for the upper limit, resulting in a temperature range of 29.5 ℃, which is 64.1 % of the specified TMH 7 range for a 50-year return period.

An overestimation of the design AAT limits (and consequently the EBT limits) could lead to an unwarranted reduction in the overall bridge length. This would result from exaggerated assumptions of deck movement, which in turn cause an overestimation of the backfill soil pressures acting behind the abutments.

From the descriptive statistics in **Table 2**, it can be seen that the EBT had the least amount of variation in the winter months despite the ambient temperature having the most variation during the same period. This is due to the shorter solar days, lower solar radiation and low wind speeds during

winter (Skorpen, 2020). The shorter solar days and lower solar radiation results in less heat energy being transferred to the bridge deck and the low wind speed facilitates low convection rates and therefore slower heat loss. Along with the thermal inertia of the bridge deck making it less susceptible to environmental changes, this results in less variation of the EBT during winter.

CORRELATION BETWEEN THE CLIMATE AND EFFECTIVE BRIDGE TEMPERATURE

The claim from Black et al. (1976) stating that the mean pentads of the EBT are identical to that of the AAT was investigated and applied to the VZ dataset. The data from the VZ bridge considered for the calculations were recorded after the deck has been surfaced in August 2017, as shown in **Fig. 12**. Comparing the mean pentad values of VZ to that in the UK as previously shown in **Fig. 1** it can be seen that that the AAT mean pentads exceeded 20 °C during the summer whereas in the UK it was below 20 °C, as a result of the differences in environments between central South Africa and the UK.

The results of the correlation between the AAT and EBT mean pentads are displayed in **Fig. 13 (a)**. The data from Black et al. (1976) is also shown in the figure. Both datasets were found to have statistically significant correlations between the EBT mean pentads and AAT mean pentads with correlation coefficients (c) of 0.93 and 0.97 for the VZ and Black et al. (1976) datasets, respectively, with both correlation coefficients obtaining p-values $<< 0.05$ indicating that the linear correlations were not arbitrarily obtained. However, although strong linear correlations exist, the original statement by Black et al. (1976) stated that the values between the EBT mean pentads and AAT mean pentads were identical. Therefore, a two-tailed t-test on the difference in means between the EBT mean pentads and AAT mean pentads for each dataset was performed. For the Black et al. (1976) dataset, the test produced values of $t = 0.07$ and $p = 0.94$. Therefore, the null hypothesis stating that there is no difference between the means of the EBT mean pentads and AAT mean pentads cannot be rejected, indicating that their statement was indeed correct. However, the hypothesis test performed on the VZ dataset yielded $t = 8.97$ and $p = 2.10e\text{-}18$, resulting in a rejection of the null hypothesis. This indicates that the mean pentads approach is not applicable to all concrete bridges as was originally assumed by Black et al. (1976) and cannot unconditionally be used to determine EBTs for setting expansion joints. The reason for the difference in results are likely to be caused by differences in environmental conditions, however, upon further investigation of the data obtained from Black et al. (1976) it was determined that the difference

was most likely caused by an over estimation of the coefficient of thermal expansion. The temperatures from Black et al. (1976) were back calculated from deck expansion (and not obtained from temperatures measured from within the bridge deck), assuming a coefficient of thermal expansion of 12 x10^{-6}/°C for concrete bridge decks. A more appropriate concrete thermal expansion coefficient would be 9 x10^{-6}/°C corresponding to concrete made with limestone aggregate (Newman and Choo, 2003). It is worth mentioning that the substantial change in thermal expansion coefficient (25 % decrease) is since historically it was common practice assuming that concrete had a similar thermal expansion coefficient than steel, which is 12 x10^{-6}/°C, however, concrete's thermal expansion coefficient may be substantially lower. Since thermal expansion is directly proportional to the product of temperature change and the coefficient of thermal expansion, it is possible to adapt the data from Black et al. (1976). The results of the α-adjusted temperatures are shown in **Fig. 13 (b)**. From the figure it is evident that the correlation between the EBT mean pentads and the AAT mean pentads is sensitive to the thermal expansion coefficient of the concrete. Since the adapted magnitude of α is similar to the measured α-value of the VZ bridge, it can be seen from the figure that the α-adjusted data from Black et al. (1976) more closely correspond to that of the VZ bridge. This showcases the importance of using appropriate measured material properties for thermal response calculations.

From **Fig. 10** it can be seen that the VZ dataset spans over a much larger range of temperatures and experiences higher peak temperatures than the data from Black et al. (1976). It can further be seen from **Fig. 10** that from spring to autumn, the EBT is substantially higher than the AAT, which agrees with the findings of Roberts-Wollman et al. (2025). It would therefore be prudent to investigate the correlation between the EBT and AAT according to season. The temperature distributions per season are shown in **Fig. 14**. From the distributions it can be seen that the EBT tends to be higher than the AAT, as is expected. Hypothesis testing confirmed that the EBT is higher than the AAT with statistical significance. The test-statistics (t) comparing the EBT with AAT were 105.5, 61.3, 32.4 and 75.1 for summer, autumn, winter and spring, respectively, with $p << 0.05$ for each season.

Fig. 15 shows the calculated EBT and recorded ambient temperature aggregated per season and averaged quarter hourly. The individual figures present a typical representation of the temperature change in a day during each season. For the summer months it seems that there is considerable overlap

between the EBT and the ambient temperature from 11:00 to 15:00. The descriptive statistics for this subset of the data in the summer is shown in **Table 3**, and was used for calculations in hypothesis testing. The null hypothesis (H_0) states that no significant difference exists between the EBT and ambient temperature distributions during summer months from 11:00 to 15:00. The two-tailed test yielded a test statistic of t = 7.92 and a p-value of 2.48×10^{-15}. Given the large data variation, the null hypothesis was rejected using a 95% significance level ($\alpha = 0.05$), indicating a statistically significant difference between EBT and ambient temperature despite the apparent temperature overlap and a difference of 0.3 ℃ between the mean values. It is therefore unlikely that the EBT would be equal to the AAT at any given time and is therefore not a suitable means for estimating bridge temperatures for maintenance purposes such as setting expansion joints and beams. This claim may further be supported by the time lag between the EBT and AAT (which is visually evident in **Fig. 15**) due to the thermal inertia of the bridge deck. If expansion joints are set based on air temperature instead of the true structural temperature, the bridge could later expand or contract more than expected which may lead to excessive stresses in the bridge deck or bearings, joint malfunction (gaps being too wide), or premature damage which may all result in increased maintenance needs.

The procedure for determining design minimum EBTs proposed by Emerson (1976) and used for the design of the VZ bridge was applied to the dataset acquired from field monitoring. The results were compared to those of Emerson (1976) and is displayed in **Fig. 16**. From the figure it can first be seen that the correlation between 24-hour minimum EBT and 48-hour mean AAT obtained from Emerson (1976) fits well within the VZ dataset's 95% confidence interval. It can also be seen that for a given 24-hour minimum AAT, the climate near the VZ bridge experiences higher 48-hour mean AATs than that of Emerson (1976), i.e., in the UK. It can further be noted that there is a linear correlation between the 24-hour minimum AAT and 48-hour mean AAT as opposed to Emerson's nonlinear correlation.

The design 24-hour minimum AAT, for a 50-year return period, used for the VZ bridge was -13 ℃ and following the design procedure as proposed by Emerson (1976) depicted by the black arrows labelled as (1), a design minimum EBT of -8 ℃ was obtained and used for the VZ bridge. If the same design procedure is used, but on the correlations from the VZ data, denoted by (2), it can be seen that

the obtained design minimum EBT is -2 ℃. However, from the analysis of the measured EBT data, the true 50-year return period for minimum EBT was calculated as 4.3 ℃, as indicated by the green star on the x-axis on the left-hand side of **Fig. 16**. It is clear that using the environmental correlations obtained from the colder UK climate, the design minimum EBT was over-estimated by 12.3 ℃ - using procedure (1). However, when using the correlations of the VZ dataset it can be seen that procedure (2) over-estimated the design minimum EBT by 6.3 ℃. The reason is because the 24-hour minimum AAT for a 50-year return period was calculated as -1.4 ℃ from the meteorological data and not -13 ℃ as assumed for the design of the VZ bridge. In procedure (3), when the correct 24-hour minimum AAT for a 50-year return period is used, the corresponding minimum EBT obtained is 8.5 ℃. This procedure under-estimates the true 50-year return period for minimum EBT by 4.2 ℃. The mismatch occurs despite using true correlations from the measured VZ bridge data because the linear regression captures only the average relationship between the 24-hour minimum AAT and the 48-hour mean AAT, not the relationship between the extremes, which is the focus of this analysis.

Fig. 17 shows a proposed method to remedy the mismatch between the 50-year return period for minimum EBT. Since the extreme values are sought instead of average behaviour it would be prudent to use the extreme values of the VZ dataset. **Fig. 17** shows the band that contains 95 % of the measured VZ bridge data, and if the lower edge of the band is used instead of the regression line used previously, it can be seen from the procedure depicted by the red dash-dot line, that the correct minimum EBT for a 50-year return period was obtained. The procedure outlined in **Fig. 17** may be adapted to appropriate meteorological data obtained from a region where a bridge is to be designed in order to obtain reasonable design minimum EBTs.

This design procedure has been extended to be applied to obtaining the design maximum EBT as shown in **Fig. 18**. This procedure relates the 24-hour maximum AAT to the 48-hour mean AAT from which the design maximum EBT could be determined. However, it should be noted that the 95% range of the VZ dataset relating the 24-hour maximum AAT to the 48-hour mean AAT is not a linear range. The 95% range was determined for each 1 ℃ increment of 24-hour maximum AAT, which resulted in a nonlinear band that encompasses the data. It should further be noted that the upper bound of the 95% range was used instead of the mean line for determining the 48-hour mean AAT associated with the 24-

hour maximum AAT, since the mean line is not appropriate for estimating extreme temperature values. Applying the proposed method as indicated by the red line in **Fig. 18** the 50-year return period maximum AAT of 32.7 ℃ results in a design maximum EBT of 33 ℃ which differs 0.8 ℃ from the actual 50-year return period maximum EBT of 33.8 ℃ as indicated by the green star on the x-axis of the left-hand figure. If a linear band for the 95% range was used it would result in a substantial over-estimation of the design maximum EBT by approximately 5 ℃. Therefore, a more refined band that narrows at the ends of the data distribution was adopted. There are more variables that influence the 24-hour maximum AAT, such as cloud cover, wind chill, peak solar radiation and solar day length whereas with the 24-hour minimum AAT, less variables influence the magnitude since it is governed by nighttime where conditions remain relatively unchanged.

Although strong correlations between EBT and AAT were observed, the assumption that their mean values are identical was not consistently supported. It was found that the EBT typically exceeds AAT and that differences in environmental conditions and material properties, particularly the thermal expansion coefficient, significantly influenced results. Existing design methods were found to over- or underestimate critical temperature values, suggesting that region-specific data and updated statistical approaches are necessary for accurate thermal design of bridges.

CONCLUSIONS

This study evaluated the long-term thermal response of the Van Zylspruit Bridge, a reinforced concrete twin spine-beam bridge located in central South Africa, using nine years of field data and local meteorological records. The importance of using appropriate measured thermal material properties and meteorological data was highlighted in the investigations on the correlations between the environment and bridge thermal response. The following conclusions were derived from these correlations:

1. It is highly probable that that the EBT will be higher than the AAT, therefore making it unlikely that their values would be equal at any given point in time. For general structural cases it is important to know the effective temperature of the structure at a specific point in time for maintenance purposes regarding expansion joints and bearings.
2. The design temperatures for the AAT and the EBT used for the Van Zylspruit bridge were conservative. As a result, this led to conservative limitations regarding the total length of the

bridge, due to excessive assumed deck displacements causing over-estimation of backfill soil pressures behind the abutments.

3. The Van Zylspruit bridge serves as a reference for similar environmental conditions around the world at a latitude close to -29.99° S. Although no clear change in the environmental conditions was observed, i.e., global warming, the Van Zylspruit bridge further serves as a reference to severe environmental exposures for other locations across the world where an increase in severity of environmental conditions may be expected.
4. The importance of using appropriate environmental conditions for bridge design temperatures was showcased when comparing central South African meteorological conditions to that in the UK. With the recent advancements in technology, it has become possible to collect vast amounts of data via structural health monitoring, making it a viable option to analyse local environmental data for making more accurate design assumptions.
5. Appropriate coefficients of thermal expansion of concrete should be used when investigating the thermal response of bridges. This is especially relevant to integral bridges since thermal response governs the maximum achievable length of the bridge, as well as the amount of movement in the deck, which in turn affects backfill pressures behind the abutments which may lead to possible soil-ratcheting. This is further applicable to structures in general when considering expansion joint and bearing movements.
6. An adapted method for determining design bridge temperatures was proposed, making use of locally available meteorological data to determine design bridge temperatures. This enables designers to determine:
    - more appropriate deck movements which in turn allows for longer bridge lengths,
    - determine more appropriate backfill soil pressures, and
    - more efficient maintenance procedures.

This study advances the understanding of bridge thermal response by showing that the EBT consistently exceeds the AAT, emphasizing the importance of measured thermal properties and local

climate, and by proposing a practical method to derive design temperatures from regional meteorological data.

DATA AVAILABILITY STATEMENT

Some or all data, models, or code that support the findings of this study are available from the corresponding author upon reasonable request.

ACKNOWLEDGEMENTS

Field monitoring was supported by the South African National Roads Agency SOC Ltd, Mott Macdonald PDNA, Aveng Grinaker LTA, and the SANRAL RFA 7a2 Integral Bridge Research Team.

REFERENCES

Black, W., Moss, D., and Emerson, M. (1976). Bridge temperatures derived from measurement of movement. Report No. LR748, Transport and Road Research Laboratory, Crowthorne, Berkshire. Available at: https://www.trl.co.uk/uploads/trl/documents/LR748.pdf [Accessed 30 April 2025].

BSI (British Standards Institution). (1978). *Steel, concrete and composite bridges.* Part 2: Specification for loads. British Standards BS 5400.

Dreyer, T., Fronek, A., Fataar, H., Mpye, G., Skorpen, S., Kearsley, E., and van Zijl, G. (2025). Soil-structure interaction analysis of transition zone deformations due to imposed abutment displacement cycles in an integral bridge. *Journal of Bridge Engineering*, Vol. 30, No. 4, p. 04025005. DOI: https://www.doi.org/10.1061/JBENF2.BEENG-7034.

Elbadry, M., and Ghali, A. (1983). Nonlinear temperature distribution and its effects on bridges. *IABSE Periodicca*, Vol. 3, pp. 169 – 191.

Emerson, M. (1976). Extreme values of bridge temperatures for design purposes. TRRL Laboratory Report 744, Transport and Road Research Laboratory, Crowthorne, Berkshire. Available at: https://www.trl.co.uk/uploads/trl/documents/LR744.pdf [Accessed 30 April 2025].

Emerson, M. (1977). Temperatures in bridges during the hot summer of 1976. TRRL Laboratory Report 783, Transport and Road Research Laboratory, Crowthorne, Berkshire. Available at: https://www.trl.co.uk/uploads/trl/documents/LR783.pdf [Accessed 30 April 2025].

Emerson, M. (1980). Temperatures in bridges during the cold winter of 1978/1979. TRRL Laboratory Report 926, Transport and Road Research Laboratory, Crowthorne, Berkshire. Available at: https://www.trl.co.uk/uploads/trl/documents/LR926.pdf [Accessed 30 April 2025].

Hoffman, F., and Phares, B. (2014). Thermal load design philosophies for horizontally curved girder bridges with integral abutments. *Journal of Bridge Engineering*, Vol. 19, No. 5, p. 04014008. DOI: https://www.doi.org/10.1061/(ASCE)BE.1943-5592.0000573.

Li, L., Chen, B., Zhou, L., Xia, Q., Zhou, Y., Zhou, X., and Xia, Y. (2023). Thermal behaviour of bridges - A literature review. *Advances in Stuctural Engineering*, Vol. 26, No. 6, pp. 985 - 1010. DOI: https://www.doi.org/10.1177/13694332231153976.

Moeletsi, M., Myeni, L., Kaempffer, L., Vermaak, D., de Nysschen, G., Henningse, C., Nel, I., Rowswell, D. (2022). Climate dataset for South Africa by the Agricultural Research Council. Data, 7(8), pp. 1-7.

Morley, D., Skorpen, S., Adendorff, J., Kearsley, E., Jacobsz, S., and Madabhushi, G. (2025). Extended monitoring of earth pressures behind a 90 m integral bridge. *Journal of Bridge Engineering*, Vol. 30, No. 4, p. 04025014. DOI: https://www.doi.org/10.1061/JBENF2.BEENG-7188.

Newman, B. and Choo, B. (2003). *Advanced concrete technology: Processes*. Oxford: Elsevier Butterworth-Heinemann. ISBN: 0 7506 5105 9.

Pearson, A., Birely, A., Yarnold, M., and Hurlebaus, S. (2024). Field study of bonded link slabs subjected to ambient live and thermal loads. *Journal of Bridge Engineering*, Vol. 29, No. 6, p. 123. DOI: https://doi.org/10.1061/jbenf2.beeng-6503.

Potgieter, I., and Gamble, W. (1989). Nonlinear temperature distributions in bridges at different locations in the United States. *PCI Journal*, pp. 80 - 103. DOI: https://www.doi.org/10.15554/pcij.07011989.80.103.

Priestley, M. (1978). Design of concrete bridges for temperature gradients. *ACI Journal*, Vol. 75, No. 5, pp. 209 - 217. DOI: https://www.doi.org/10.14359/10934.

Roberts-Wollman, C., Breen, J., and Cawrse, J. (2002). Measurements of thermal gradients and their effects on segmental concrete bridge. *Journal of Bridge Engineering*, Vol. 7, No. 3, pp. 166 – 174. DOI: https://www.doi.org/10.1061/(ASCE)1084-0702(2002)7:3(166).

Saad, S., Nasir, A., Bashir, R., and Pantazopoulou, S. (2023). Numerical study on the effect of climate parameters on the extreme thermal gradients in concrete box girders. *Journal of Bridge Engineering*, Vol. 28, No. 10, p. 04023069. DOI: https://doi.org/10.1061/JBENF2.BEENG-6184.

Saad, S., Nasir, A., Bashir, R., and Pantazopoulou, S. (2025). Effect of climate change on thermal loads in concrete box girders. *Journal of Bridge Engineering*, Vol. 30, No. 3, p. 04025004. DOI: https://www.doi.org/10.1061/JBENF2.BEENG-6835.

SANS 6085:2006. (2006). Concrete tests – Initial drying shrinkage and wetting expansion of concrete, SABS 6085, South African Bureau of Standards, Pretoria.

Skorpen, S., Kearsley, E., and Clayton, C. (2019). Structural health monitoring of an integral bridge. In: *International Conference on Smart Infrastructure and Construction (ICSIC) 2019: Driving data-informed decision-making*, Cambridge, UK: ICE Publishing, pp. 743 - 749. DOI: https://www.doi.org/10.1680/icsic.64669.743.

Skorpen, S., Kearsley, E., and Kruger, E. (2018). Measured temperature and shrinkage effects on a 90m long integral bridge in South Africa. *Proceedings of the Institution of Civil Engineers - Bridge Engineering*, Vol. 171, No. 3, pp. 169 - 178. DOI: https://www.doi.org/10.1680/jbren.17.00019.

Skorpen, S., Kearsley, E., Clayton, C., and Kruger, E. (2020). Structural monitoring of an integral bridge in South Africa. *Proceedings of the Institution of Civil Engineers - Smart Infrastructure and Construction*, Vol. 173, No. 3, pp. 63 - 72. DOI: https://www.doi.org/10.1680/jsmic.20.00001.

Skorpen, S. (2020). Temperature effects and the behaviour of long reinforced concrete integral bridges, PhD Thesis. Pretoria, South Africa: University of Pretoria.

Song, X., Melhem, H., Li, J., Xu, Q., and Cheng, L. (2016). Effects of solar temperature gradient on long-span concrete box girder during cantilever construction. *Journal of Bridge Engineering*, Vol. 21, No. 5, p. 04015061. DOI: https://www.doi.org/10.1061/(ASCE)BE.1943-5592.0000844.

TMH 7. (1989). *Code of practice for the design of highway bridges and culverts in South Africa*, Parts 1, 2 and 3. Department of Transport, Pretoria, South Africa.

Zhou, Y., Xia, Y., and Fujino, Y. (2021). Analytical formulas of beam deflection due to vertical temperature difference. *Engineering Structures*, Vol. 240, p. 112366. DOI: https://www.doi.org/10.1016/j.engstruct.2021.112366.

LIST OF TABLES

Table 1. Descriptive statistics of the environmental conditions

Environmental Parameter	Season	Count	Min	25 %	Mean	95 %	Max	Standard Deviation	COV
Ambient Air Temperature [°C]	All	76 398	-10.0	9.7	15.5	29.5	39.9	8.3	0.54
	Summer	19 498	2.5	16.4	21.3	32.2	39.9	6.3	0.30
	Autumn	19 870	-6.2	10.2	15.0	26.4	35.2	6.8	0.45
	Winter	18 360	-10.0	3.4	8.6	19.9	27.8	6.7	0.79
	Spring	18 670	-7.9	11.2	16.9	30.0	37.2	7.8	0.46
Solar Radiation [W/m^2]	All	76 399	0	0.029	241	931	1 219	327	1.37
	Summer	19 499	0	0.033	309	1 039	1 219	380	1.23
	Autumn	19 870	0	0.026	204	803	1 092	288	1.41
	Winter	18 360	0	0.026	169	658	881	242	1.44
	Spring	18 670	0	0.031	281	976	1 182	358	1.27
Wind Speed [m/s]	All	76 388	0	1.4	3.0	7.2	15.1	2.2	0.73
	Summer	19 500	0	1.5	3.2	7.3	11.7	2.2	0.69
	Autumn	19 870	0	1.3	2.7	6.4	11.1	1.9	0.70
	Winter	18 357	0	1.6	3.0	7.2	15.1	2.1	0.70
	Spring	18 661	0	1.4	3.2	7.7	13.4	2.4	0.75
Hourly Relative Humidity [%]	All	74 346	5.0	28.4	50.5	94.2	100	25.8	0.51
	Summer	18 934	5.0	28.6	51.8	95.0	100	26.7	0.52
	Autumn	19 060	8.0	38.5	58.8	96.2	100	24.0	0.41
	Winter	18 004	5.8	30.6	50.5	92.1	100	23.7	0.47
	Spring	18 348	5.0	19.1	40.6	89.1	100	25.3	0.62
Seasonal Rainfall [mm]	Summer	271	80	134	189	299	305	78	8.62
	Autumn	201	0	110	138	229	264	70	8.28
	Winter	71	0	2	29	71	75	28	14.42
	Spring	110	0	14	77	226	291	89	13.45

Table 2. Descriptive statistics of the Effective Bridge Temperature

Season	Count	Min [°C]	25 % [°C]	Mean [°C]	95 % [°C]	Max [°C]	Standard Deviation [°C]	COV
All	285 144	2.6	12.6	19.1	29.8	36.5	7.2	0.38
Summer	66 053	17.3	24.6	26.7	31.8	36.5	3.1	0.12
Autumn	67 839	6.3	14.7	18.6	26.8	32.3	4.9	0.26
Winter	75 924	2.6	8.4	10.3	15.1	20.7	2.7	0.26
Spring	75 328	8.4	18.2	21.7	29.3	35.0	4.6	0.21

Table 3. Descriptive statistics for hypothesis testing

	Count	**Mean [°C]**	**Standard Deviation [°C]**	**COV**
Daily temperature distribution during Summer between 11:00 and 15:00 (**Fig. 15**)				
Effective Bridge Temperature	13 763	26.4	2.74	0.10
Ambient Air Temperature	12 721	26.7	3.41	0.13

Figure 1

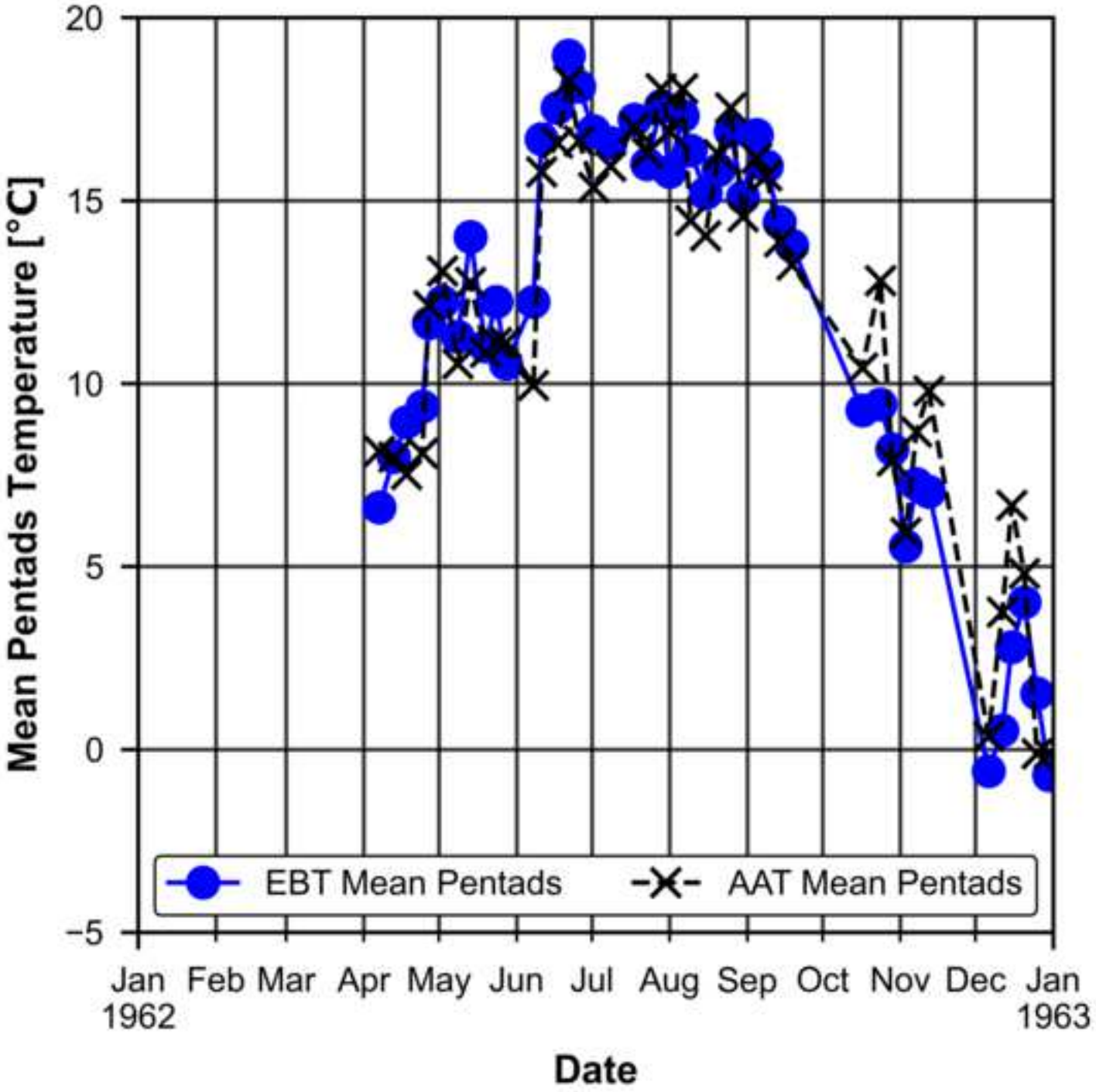
20
15
10
5
0
−5
Mean Pentads Temperature [°C]
EBT Mean Pentads
AAT Mean Pentads
Jan
1962
Feb
Mar
Apr
May
Jun
Jul
Aug
Sep
Oct
Nov
Dec
Jan
1963
Date

Figure 2

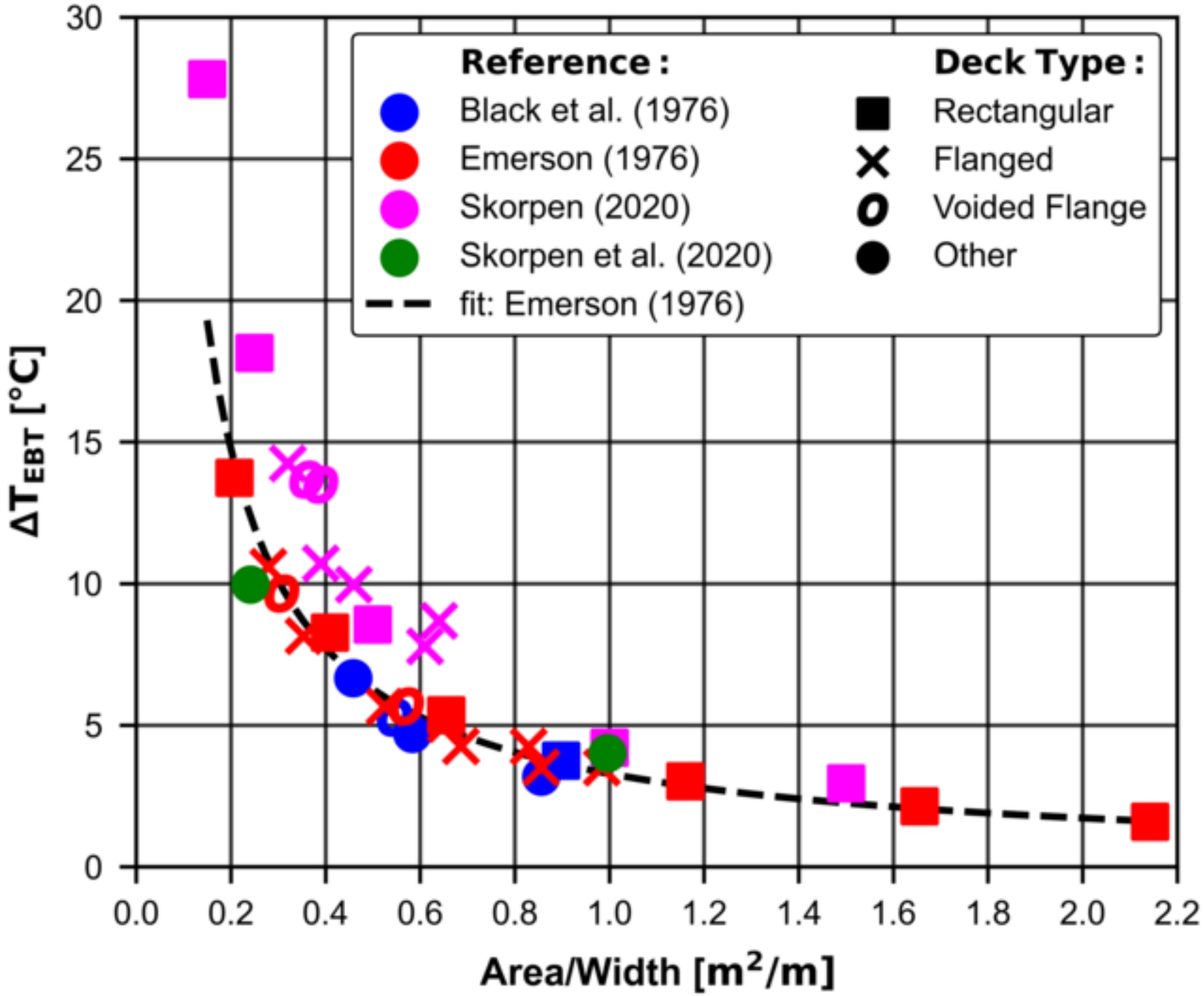
Reference :
Black et al. (1976)
Emerson (1976)
Skorpen (2020)
Skorpen et al. (2020)
fit: Emerson (1976)
Deck Type :
Rectangular
Flanged
Voided Flange
Other
ΔT_EBT [°C]
Area/Width [m²/m]
0
5
10
15
20
25
30
0.0
0.2
0.4
0.6
0.8
1.0
1.2
1.4
1.6
1.8
2.0
2.2

Figure 3

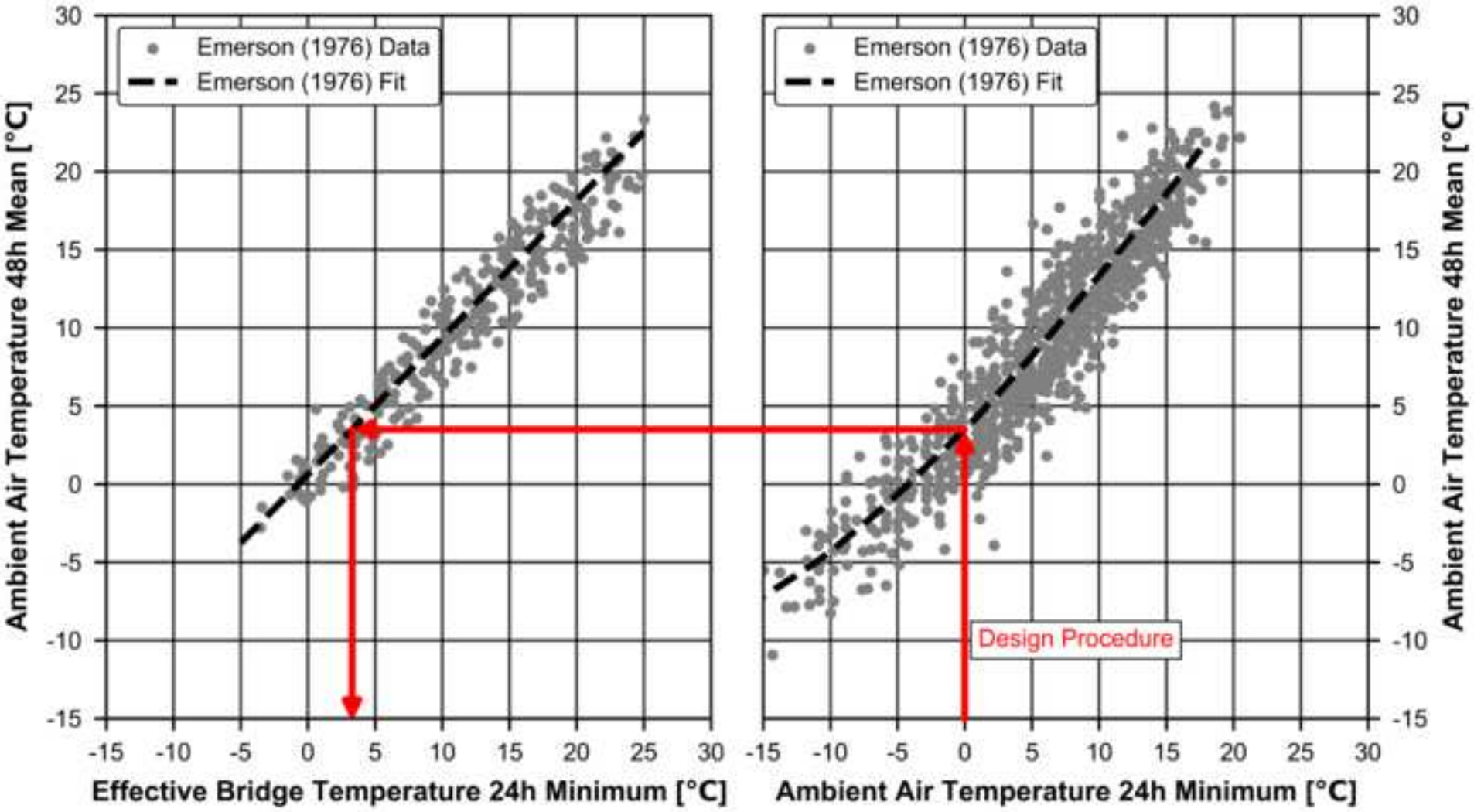
Emerson (1976) Data
Emerson (1976) Fit
Ambient Air Temperature 48h Mean [°C]
Effective Bridge Temperature 24h Minimum [°C]
Emerson (1976) Data
Emerson (1976) Fit
Design Procedure
Ambient Air Temperature 24h Minimum [°C]
Ambient Air Temperature 48h Mean [°C]

Figure 4

Figure 5a

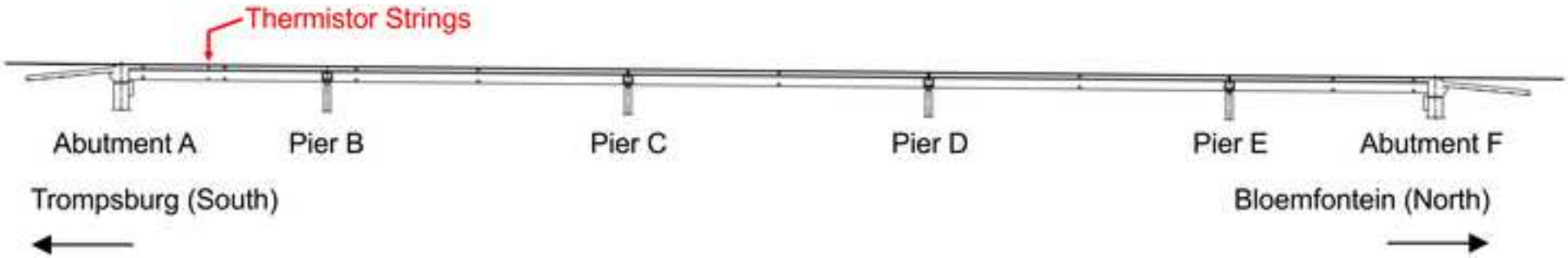
Thermistor Strings
Abutment A
Pier B
Pier C
Pier D
Pier E
Abutment F
Trompsburg (South)
Bloemfontein (North)

Figure 5b

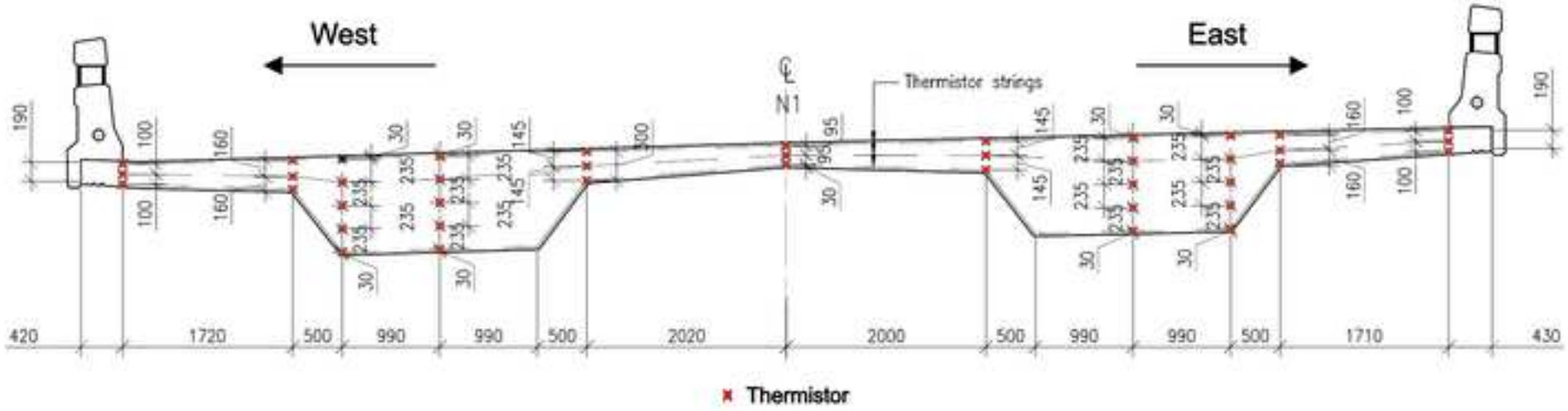
West
East
Thermistor strings
N1
190
100
160
30
235
145
300
95
420
1720
500
990
990
500
2020
2000
500
990
990
500
1710
430
Thermistor

Figure 6

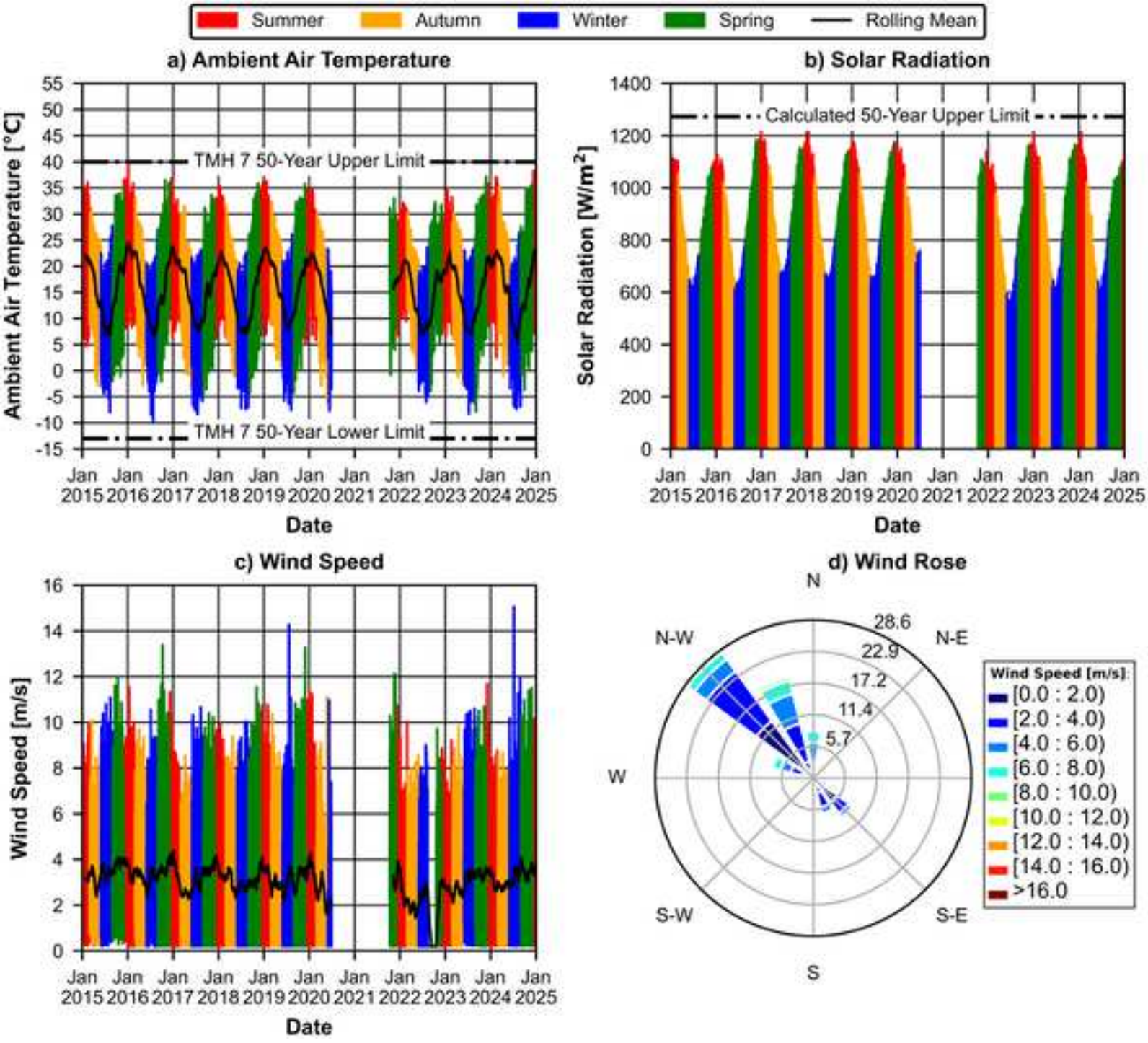
Summer
Autumn
Winter
Spring
Rolling Mean
a) Ambient Air Temperature
Ambient Air Temperature [°C]
TMH 7 50-Year Upper Limit
TMH 7 50-Year Lower Limit
Date
b) Solar Radiation
Solar Radiation [W/m²]
Calculated 50-Year Upper Limit
Date
c) Wind Speed
Wind Speed [m/s]
Date
d) Wind Rose
N
N-E
E
S-E
S
S-W
W
N-W
28.6
22.9
17.2
11.4
5.7
Wind Speed [m/s]:
[0.0 : 2.0)
[2.0 : 4.0)
[4.0 : 6.0)
[6.0 : 8.0)
[8.0 : 10.0)
[10.0 : 12.0)
[12.0 : 14.0)
[14.0 : 16.0)
>16.0

Figure 7

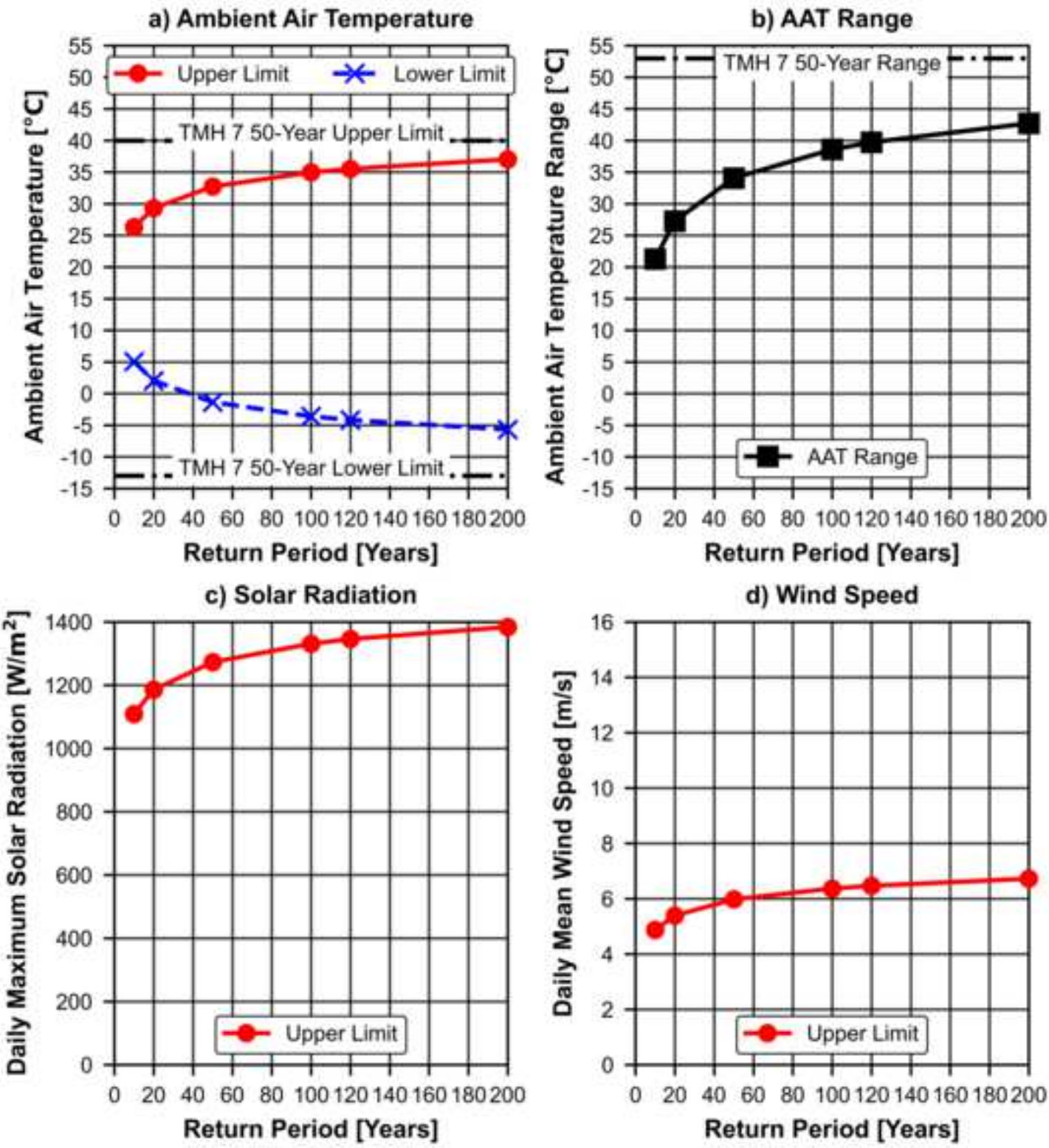
a) Ambient Air Temperature
Ambient Air Temperature [°C]
Upper Limit
Lower Limit
TMH 7 50-Year Upper Limit
TMH 7 50-Year Lower Limit
Return Period [Years]
b) AAT Range
Ambient Air Temperature Range [°C]
TMH 7 50-Year Range
AAT Range
Return Period [Years]
c) Solar Radiation
Daily Maximum Solar Radiation [W/m²]
Upper Limit
Return Period [Years]
d) Wind Speed
Daily Mean Wind Speed [m/s]
Upper Limit
Return Period [Years]

Figure 8

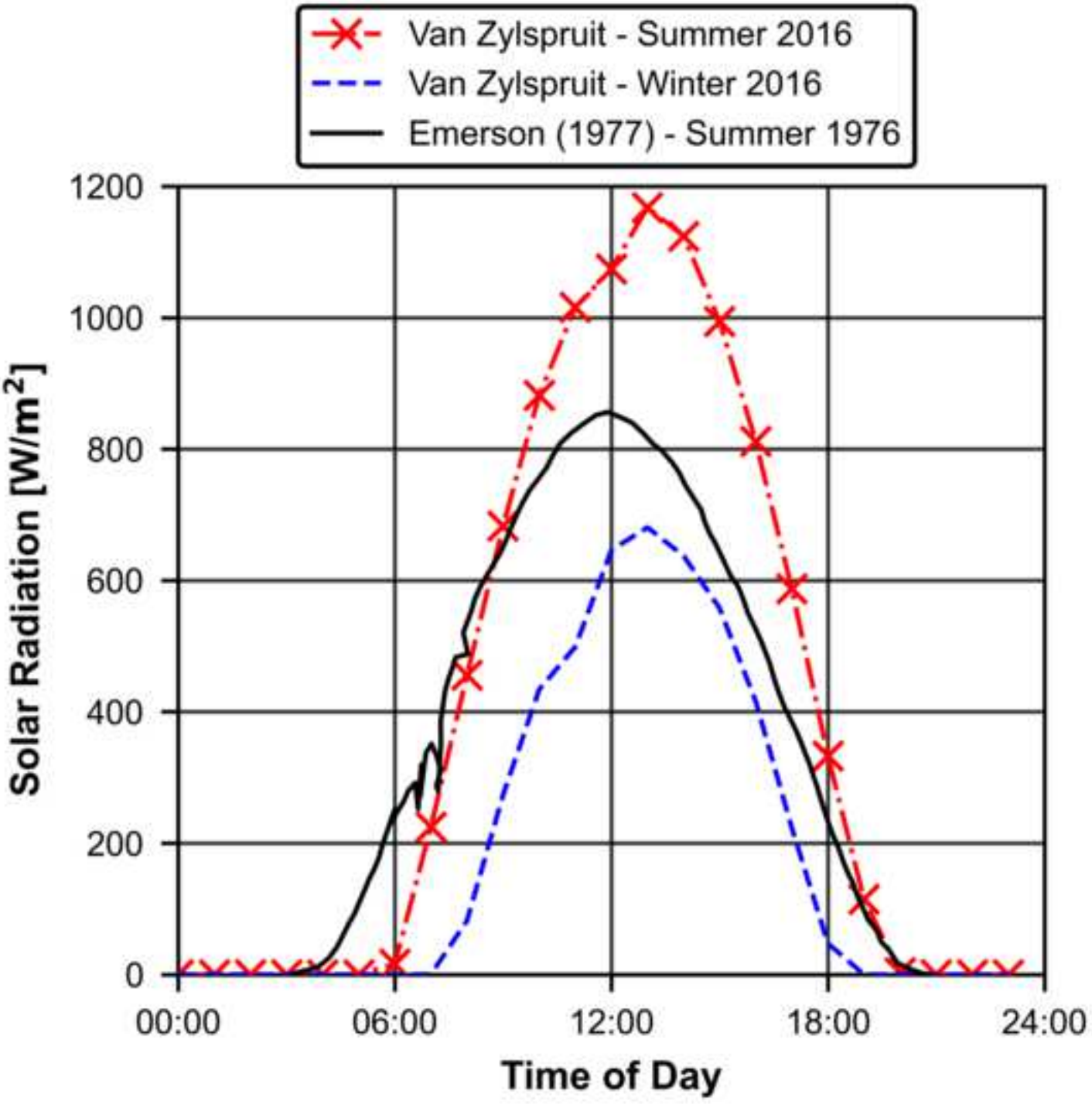
Van Zylspruit - Summer 2016
Van Zylspruit - Winter 2016
Emerson (1977) - Summer 1976
Solar Radiation [W/m²]
1200
1000
800
600
400
200
0
00:00
06:00
12:00
18:00
24:00
Time of Day

Figure 9

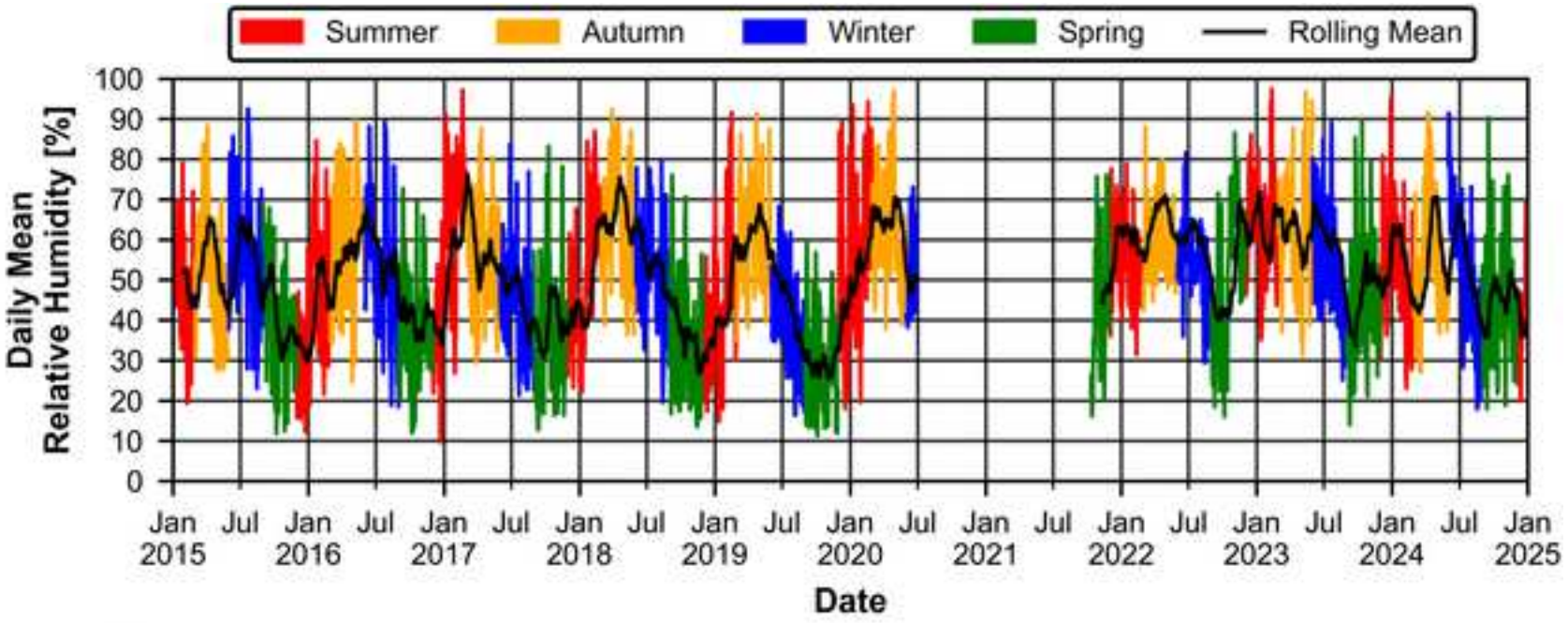

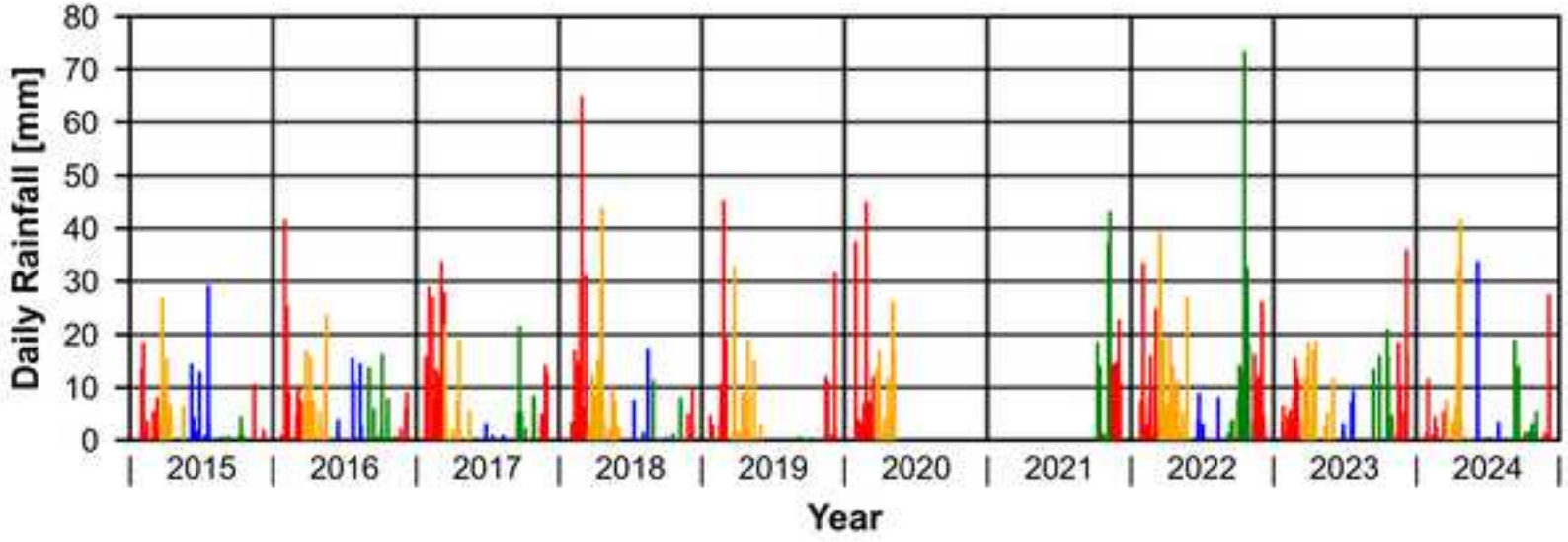

Total Yearly Rainfall [mm]	278	396	462	471	359	353	274	879	518	342
No. Rainy Days	61	76	70	67	52	48	27	116	78	58

Figure 10

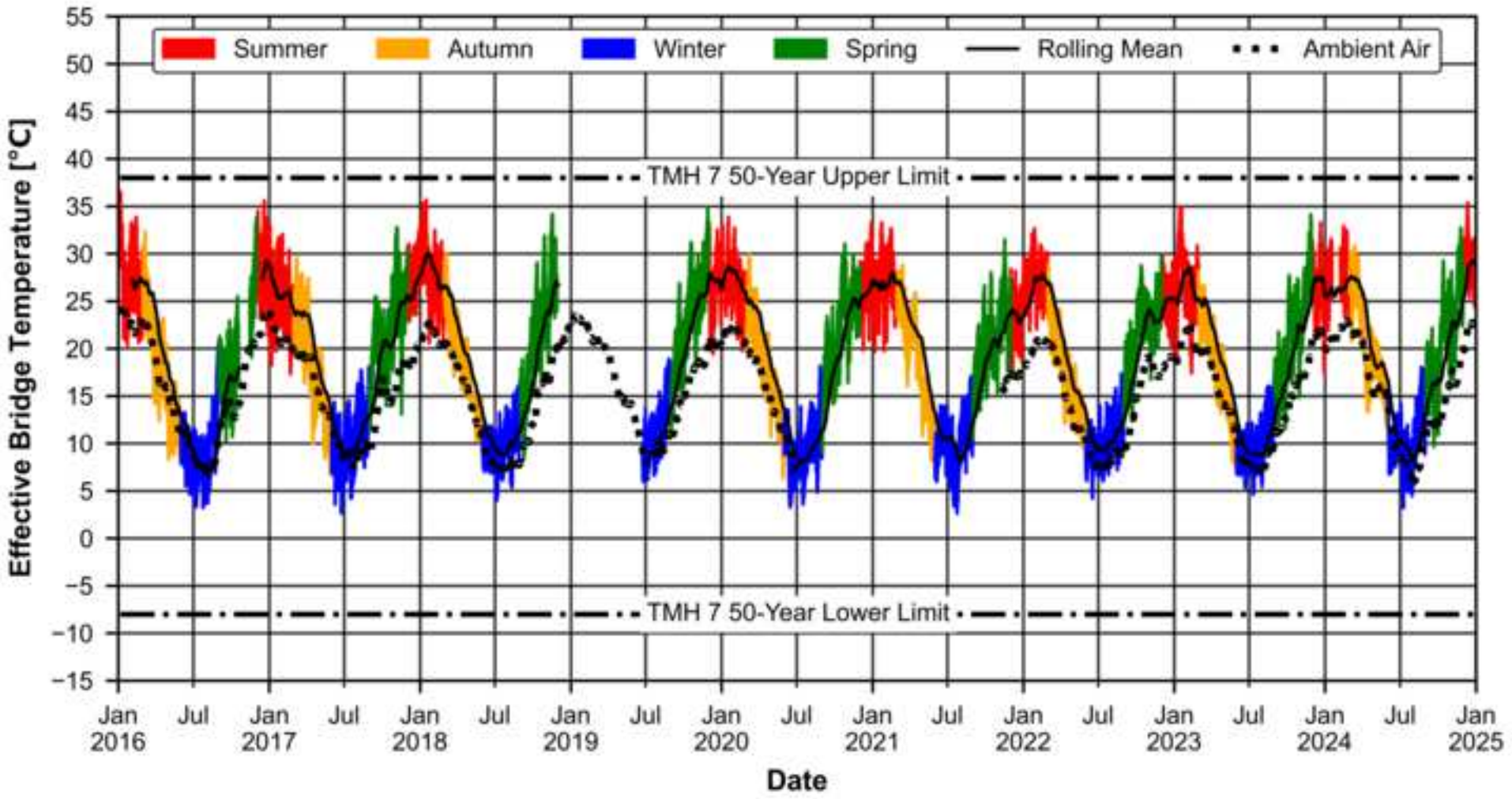
Summer
Autumn
Winter
Spring
Rolling Mean
Ambient Air
TMH 7 50-Year Upper Limit
TMH 7 50-Year Lower Limit
Effective Bridge Temperature [°C]
55
50
45
40
35
30
25
20
15
10
5
0
−5
−10
−15
Jan 2016
Jul
Jan 2017
Jul
Jan 2018
Jul
Jan 2019
Jul
Jan 2020
Jul
Jan 2021
Jul
Jan 2022
Jul
Jan 2023
Jul
Jan 2024
Jul
Jan 2025
Date

Figure 11

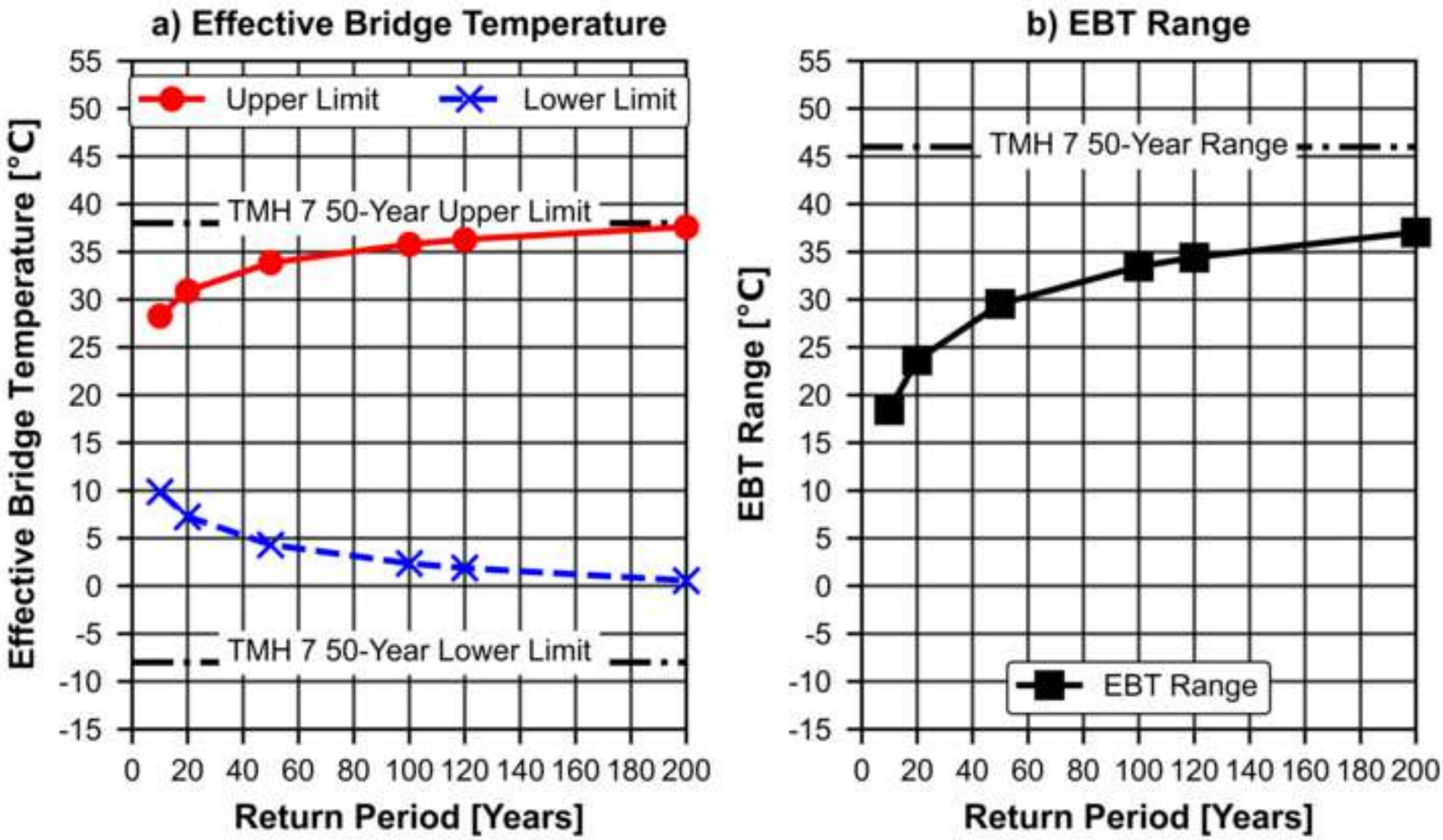
a) Effective Bridge Temperature
Effective Bridge Temperature [°C]
Upper Limit
Lower Limit
TMH 7 50-Year Upper Limit
TMH 7 50-Year Lower Limit
55
50
45
40
35
30
25
20
15
10
5
0
-5
-10
-15
0 20 40 60 80 100 120 140 160 180 200
Return Period [Years]
b) EBT Range
EBT Range [°C]
TMH 7 50-Year Range
EBT Range
55
50
45
40
35
30
25
20
15
10
5
0
-5
-10
-15
0 20 40 60 80 100 120 140 160 180 200
Return Period [Years]

Figure 12

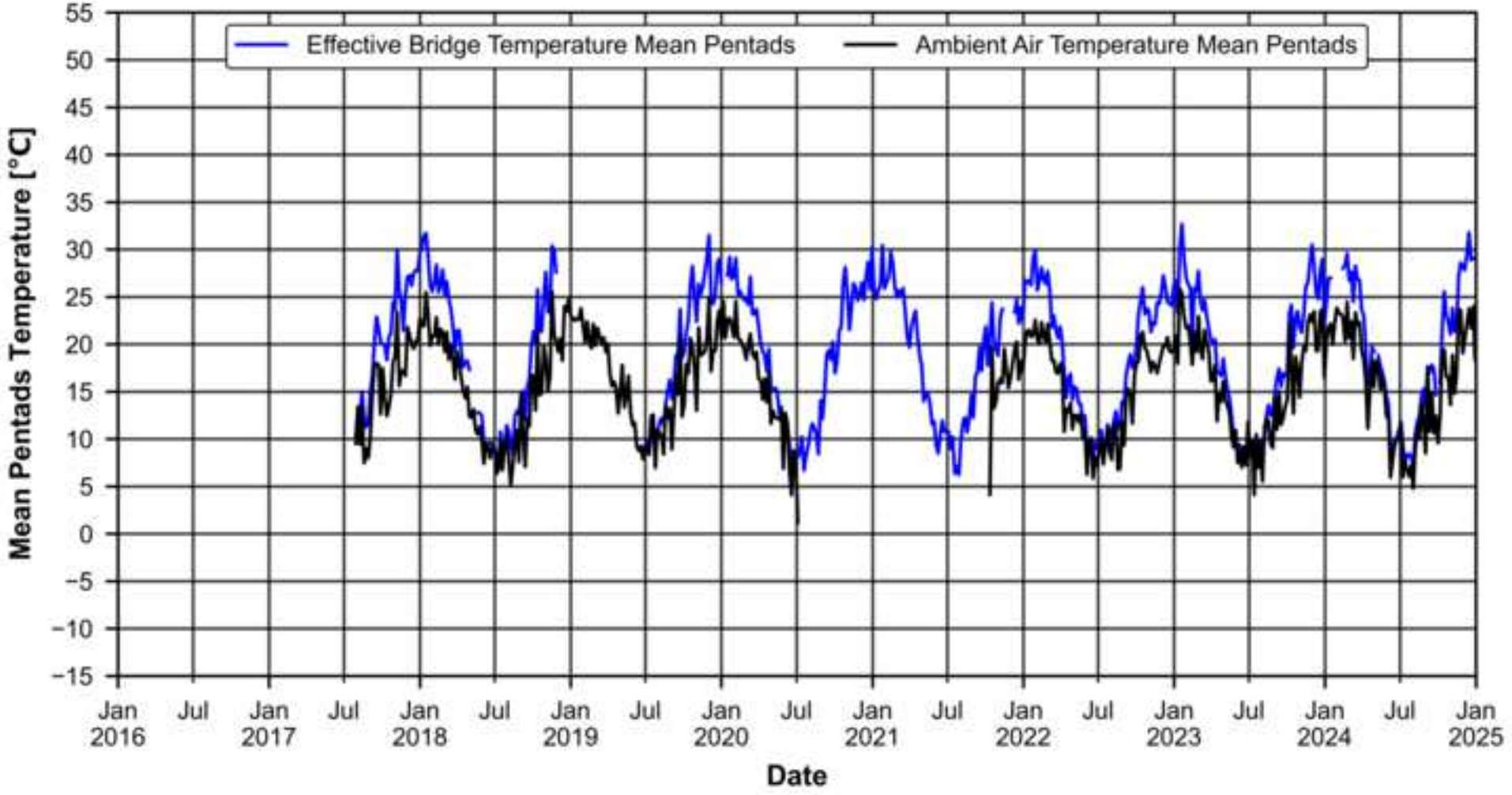
Effective Bridge Temperature Mean Pentads
Ambient Air Temperature Mean Pentads
Mean Pentads Temperature [°C]
55
50
45
40
35
30
25
20
15
10
5
0
−5
−10
−15
Jan 2016
Jul
Jan 2017
Jul
Jan 2018
Jul
Jan 2019
Jul
Jan 2020
Jul
Jan 2021
Jul
Jan 2022
Jul
Jan 2023
Jul
Jan 2024
Jul
Jan 2025
Date

Figure 13a

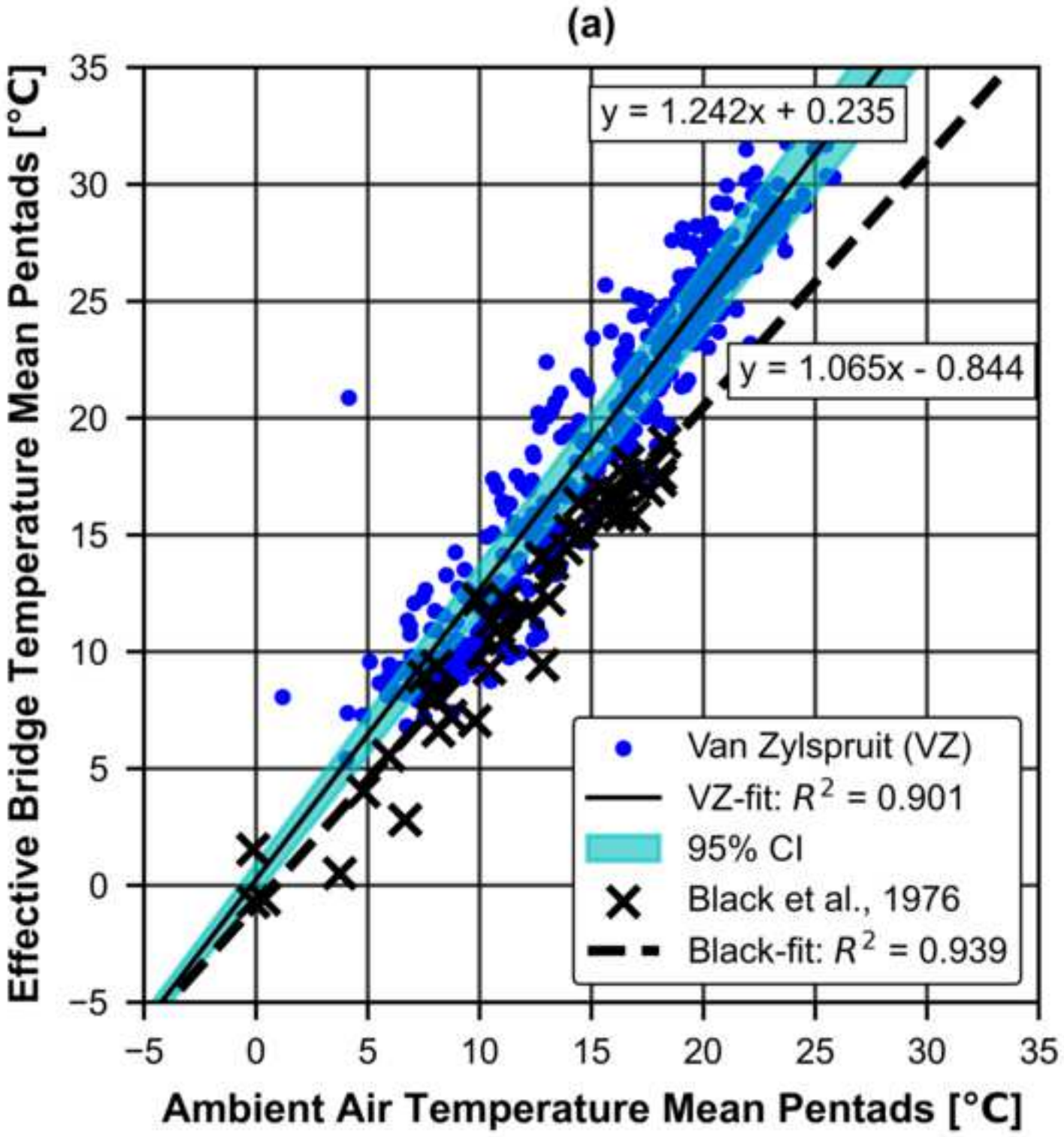
(a)
y = 1.242x + 0.235
y = 1.065x - 0.844
Van Zylspruit (VZ)
VZ-fit: R^2 = 0.901
95% CI
Black et al., 1976
Black-fit: R^2 = 0.939
Effective Bridge Temperature Mean Pentads [°C]
Ambient Air Temperature Mean Pentads [°C]
35
30
25
20
15
10
5
0
−5
−5
0
5
10
15
20
25
30
35

Figure 13b

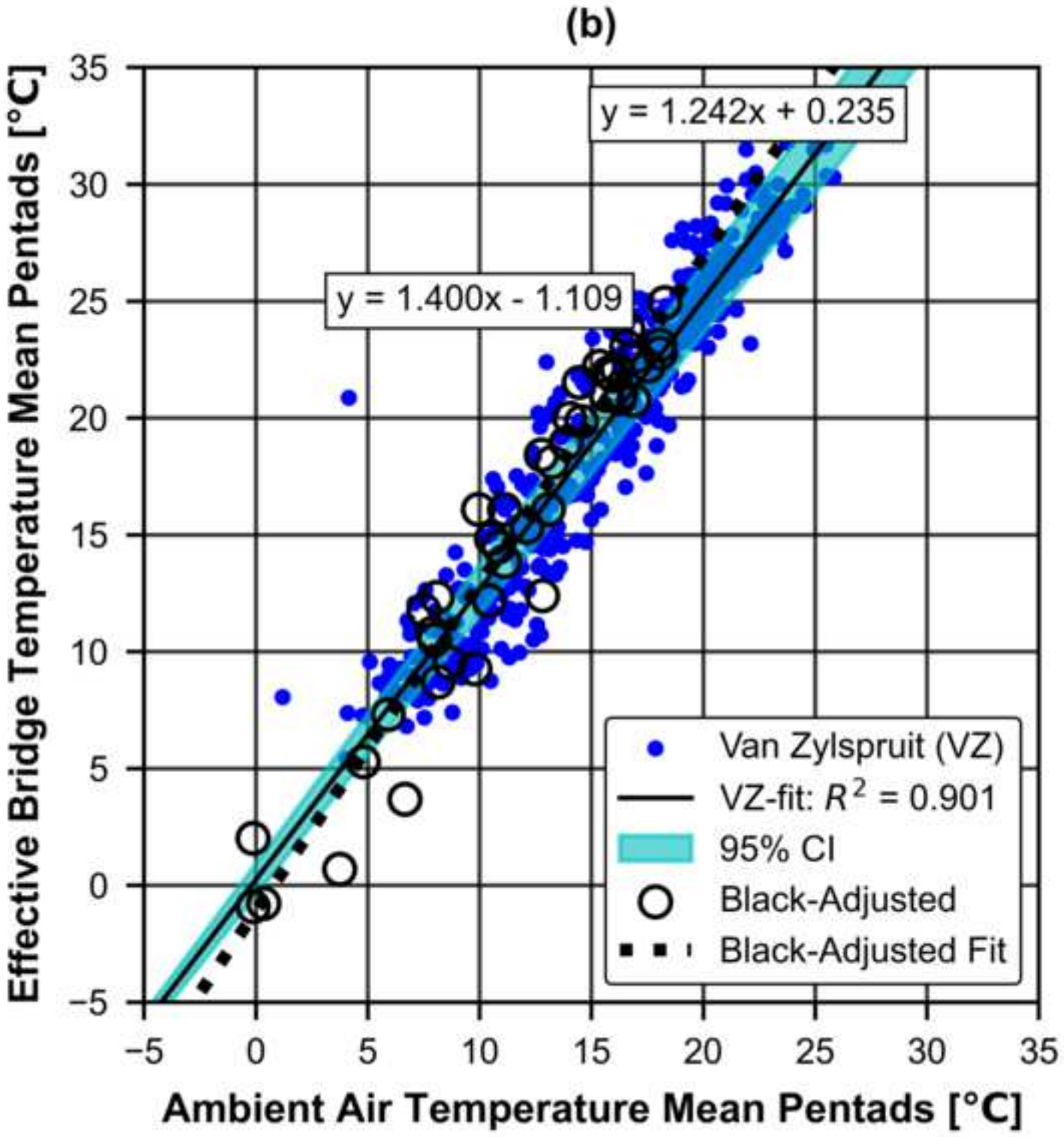
(b)
y = 1.242x + 0.235
y = 1.400x - 1.109
Van Zylspruit (VZ)
VZ-fit: R^2 = 0.901
95% CI
Black-Adjusted
Black-Adjusted Fit
Effective Bridge Temperature Mean Pentads [°C]
Ambient Air Temperature Mean Pentads [°C]
35
30
25
20
15
10
5
0
−5
−5
0
5
10
15
20
25
30
35

Figure 14

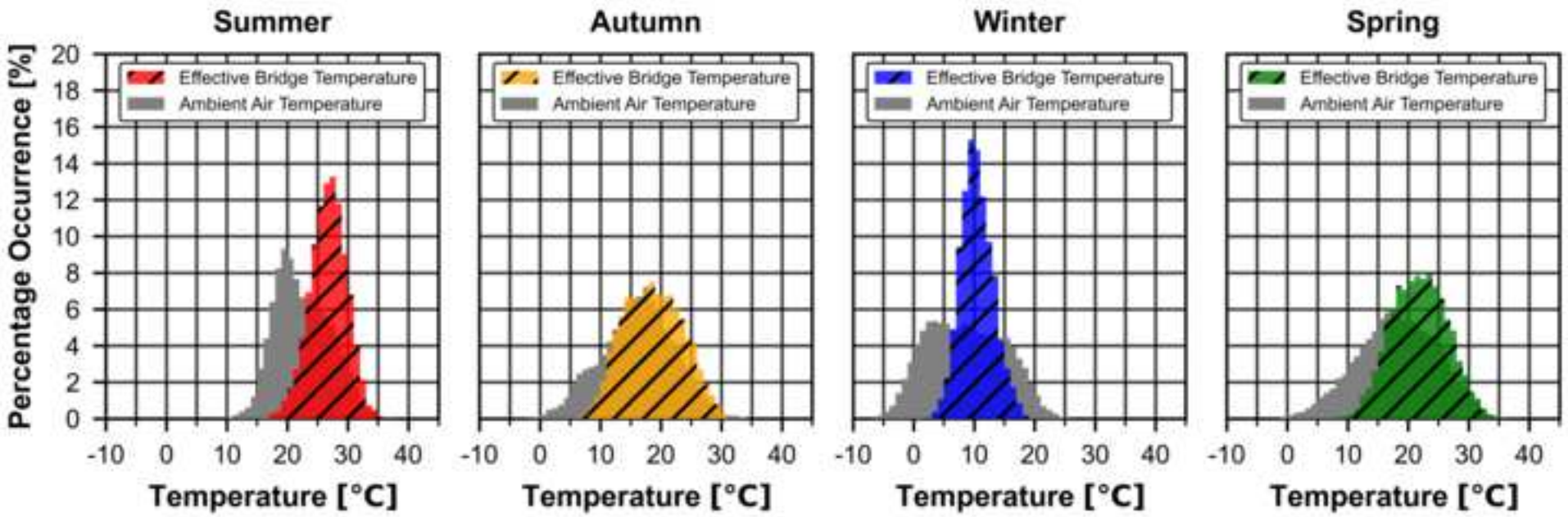
Summer
Autumn
Winter
Spring
Effective Bridge Temperature
Ambient Air Temperature
Percentage Occurrence [%]
0
2
4
6
8
10
12
14
16
18
20
-10
0
10
20
30
40
Temperature [°C]

Figure 15

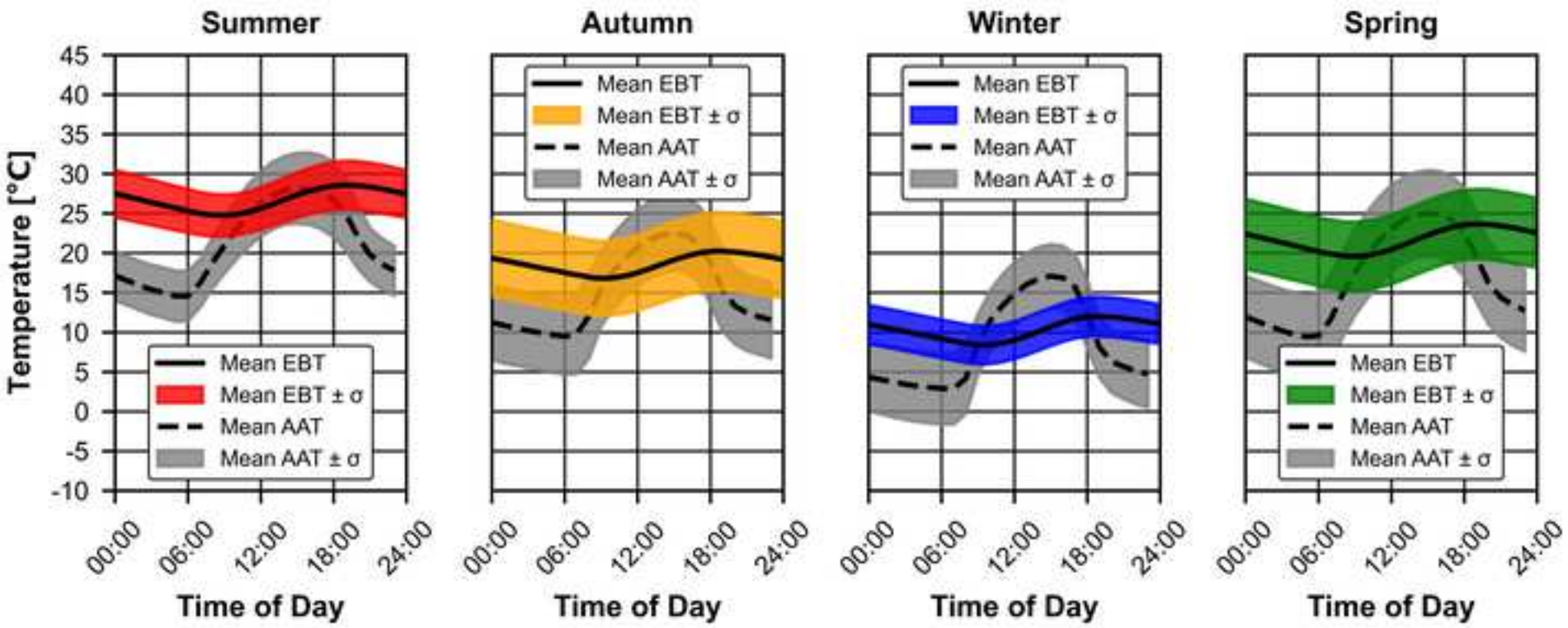
Summer
Autumn
Winter
Spring
Temperature [°C]
45
40
35
30
25
20
15
10
5
0
-5
-10
Mean EBT
Mean EBT ± σ
Mean AAT
Mean AAT ± σ
00:00
06:00
12:00
18:00
24:00
Time of Day

Figure 16

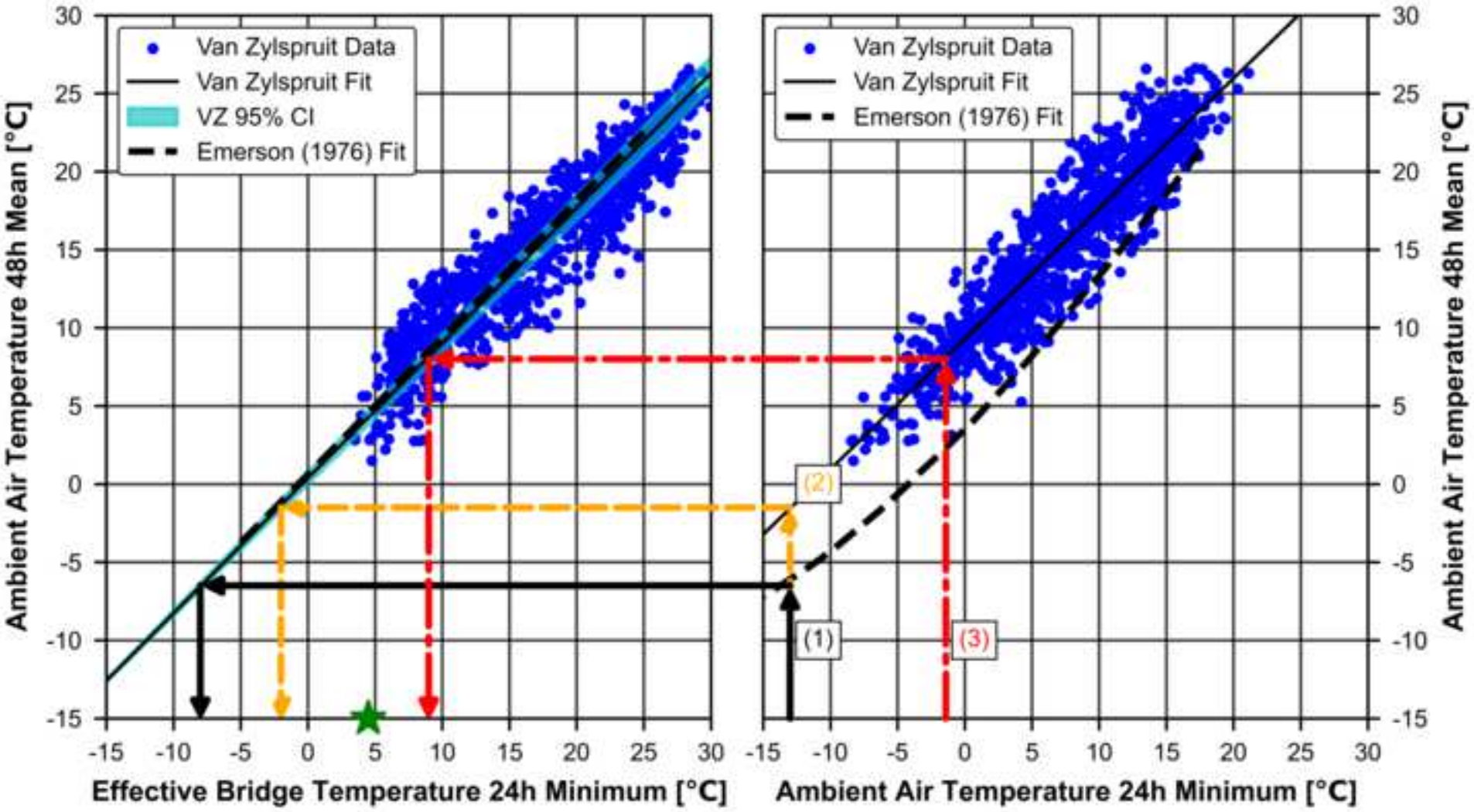
Van Zylspruit Data
Van Zylspruit Fit
VZ 95% CI
Emerson (1976) Fit
Ambient Air Temperature 48h Mean [°C]
Effective Bridge Temperature 24h Minimum [°C]
Van Zylspruit Data
Van Zylspruit Fit
Emerson (1976) Fit
Ambient Air Temperature 24h Minimum [°C]
(1)
(2)
(3)

Figure 17

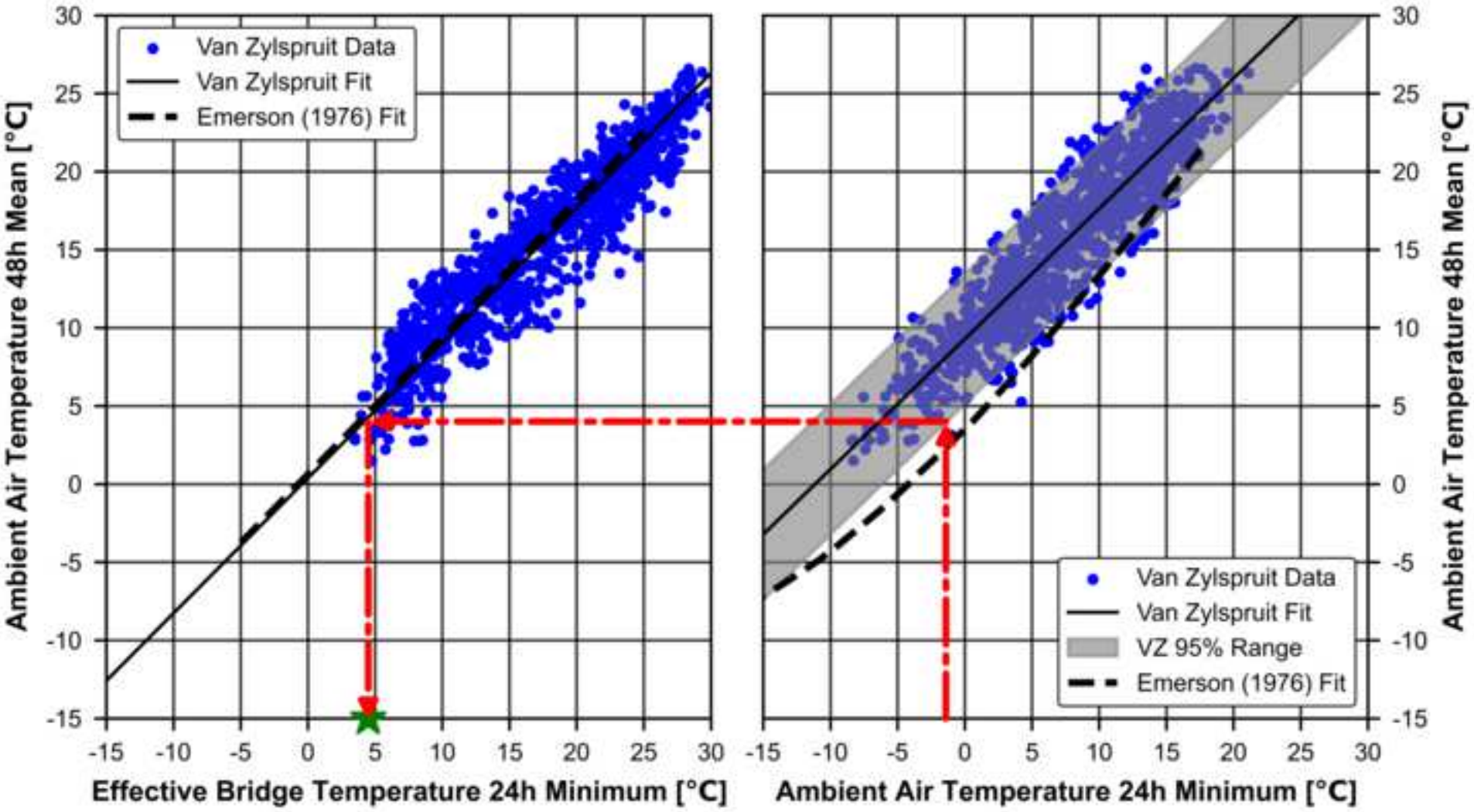
Van Zylspruit Data
Van Zylspruit Fit
Emerson (1976) Fit
Ambient Air Temperature 48h Mean [°C]
Effective Bridge Temperature 24h Minimum [°C]
Van Zylspruit Data
Van Zylspruit Fit
VZ 95% Range
Emerson (1976) Fit
Ambient Air Temperature 48h Mean [°C]
Ambient Air Temperature 24h Minimum [°C]
30
25
20
15
10
5
0
-5
-10
-15
-15 -10 -5 0 5 10 15 20 25 30

Figure 18

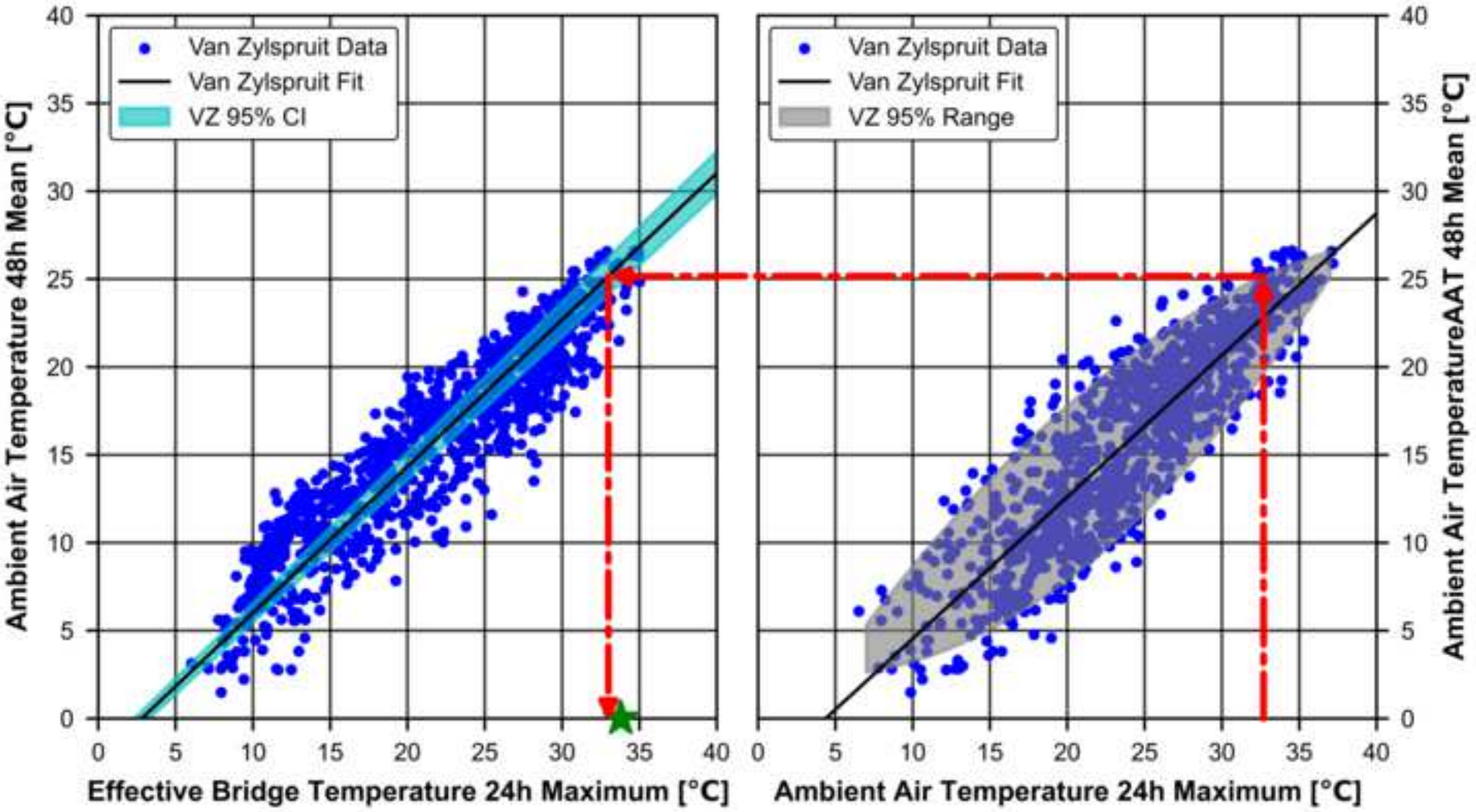
Van Zylspruit Data
Van Zylspruit Fit
VZ 95% CI
Van Zylspruit Data
Van Zylspruit Fit
VZ 95% Range
Ambient Air Temperature 48h Mean [°C]
Effective Bridge Temperature 24h Maximum [°C]
Ambient Air Temperature 24h Maximum [°C]
Ambient Air TemperatureAAT 48h Mean [°C]
0
5
10
15
20
25
30
35
40

FIGURE CAPTIONS LIST

Fig. 17. Adjusted design procedure for design minimum EBT

Fig. 18. Proposed design procedure for design maximum EBT